Reduction of perioperative inflammatory reaction with exogenous methane

Ph.D. Thesis

Gábor Bari M.D.

Supervisors: Gabriella Varga Ph.D.

Dániel Érces M.D., Ph.D.

Institute of Surgical Research

University of Szeged, Hungary

2019

LIST OF PUBLICATIONS

Full papers related to the subject of the thesis

1. **Bari G**, Érces D, Varga G, Szűcs S, Varga Z, Bogáts G, Boros M. Methane inhalation reduces the systemic inflammatory response in a large animal model of extracorporeal circulation. Eur J Cardiothoracic Surgery 2019. doi:10.1093/ejcts/ezy453. **IF: 3.5**
2. **Bari G**, Érces D, Varga G, Szűcs S, Bogáts G. A pericardialis tamponád kórélettana, klinikuma és állatkísérletes vizsgálati lehetőségei [Pathophysiology, clinical and experimental possibilities of pericardial tamponade]. Orv Hetil. 2018. 159:163–167 **IF: 0.3**
3. **Bari G**, Szűcs S, Érces D, Ugocsai M, Bozsó N, Balog D, Boros M, Varga G. A cardiogen sokk modellezése pericardialis tamponáddal [Experimental model for cardiogenic shock with pericardial tamponade]. Magy Seb. 2017. 70:297–302 **IF: 0**
4. Szűcs S, **Bari G***, Ugocsai M, Lashkarivand RA, Lajkó N, Mohácsi A, Szabó A, Kaszaki J, Boros M, Érces D, Varga G. Detection of intestinal tissue perfusion by real-time breath methane analysis in rat and pig models of mesenteric circulatory distress. Crit Care Med 2019. (*equal contribution, accepted for publication) **IF: 6.6**
5. **Bari G**, Szűcs S, Érces D, Boros M, Varga G. Experimental pericardial tamponade - translation of a clinical problem to its large animal model. Turk J Surg. 2018. 34(3):205–211 **IF: 0.1**

Abstracts related to the subject of the thesis

1. **Bari G**, Varga G, Szűcs S, Gules M, Kaszaki J, Boros M, Érces D. Methane inhalation decreases mucosal mast cell degranulation in a large animal model of cardiogenic shock. Abstract Book, 17th Congress of the European Shock Society, Paris, 13–15 September 2017.
2. **Bari G**, Érces D, Szűcs S, Gules M, Gyaraki P, Szilágyi ÁL, Hartmann P, Boros M, Varga G. Improved platelet function after methane inhalation in a large animal model of obstructive circulatory shock. Abstract Book, 53rd ESSR Congress, Madrid, 2018, p. 87 (https://www.essr2018.com/abstracts)

Full papers not related to the subject of the thesis

1. Csepregi L, **Bari G**, Bitay M, Hegedűs Z, Varga S, Iglói G, Szabó-B A, Hartyánszky I, Bogáts G. Kezdeti tapasztalatok a Sorin Perceval S aorta biológiai billentyű beültetésével [Early experiences with the Sorin Perceval S artificial biological valve]. Magy Seb. 2016. 69:54–57

2. **Bari G**, Csepregi L, Bitay M, Bogáts G. A ministernotomia szerepe az aortabillentyű-sebészetben [The role of mini-sternotomy in aortic valve surgery]. Orv Hetil. 2016. 157:901–904.

3. **Bari G**, Bogáts G, Pálinkás E, Badó A, Tiszlavicz L, Kallai A, Vörös E, Pálinkás A. Bal kamrai kompressziót okozó óriás pericardialis ciszta [Giant pericardial cyst compressing the left ventricle]. Medicina Thoracalis 2017. 70

4. Bogáts G, Hegedűs Z, Bitay M, Csepregi L, Szabó-Biczók A, Varga S, Iglói G, **Bari G**. Coronary artery bypass grafting on the beating heart: 13-year experience in a single center. J Cardiothoracic Surgery 8: S1 p. O172 (2013)

LIST OF ABBREVIATIONS

ACT	activated clotting time
ANP	atrial natriuretic peptide
CO	cardiac output
CLSEM	confocal laser scanning endomicroscope
CPB	cardiopulmonary bypass
CTMC	connective tissue mast cells
ECC	extracorporeal circulation
ECMO	extracorporeal membrane oxygenation
FcεRI	high-affinity IgE receptor
HR	heart rate
I-R	ischaemia-reperfusion
IBDs	inflammatory bowel diseases
ICAM-1	intercellular adhesion molecule 1
IgE	immunoglobulin E
Il-4	interleukin-4
Il-5	interleukin-5
MAP	mean arterial pressure
MMC	mucosal mast cells
MMP	matrix metalloproteinase
NAD^+	nicotinamide adenine dinucleotide
NOS	nitric oxide synthase
PiCCO	pulse contour cardiac output
PMN	polymorphonuclear
PT	pericardial tamponade
RA	renal artery
RAA	renin-angiotensin-aldosterone
ROS	reactive oxygen species
SIRS	systemic inflammatory response syndrome
SMA	superior mesenteric artery
TNFα	tumour necrosis factor alpha
XDH	xanthine dehydrogenase
XOR	xanthine oxidoreductase

LIST OF CHEMICAL COMPOUNDS

CH_4	methane
CO	carbon monoxide
CO_2	carbon dioxide
H_2	hydrogen
H_2S	hydrogen sulphide
NH_3	ammonia
NO	nitrogen monoxide

SUMMARY

In recent decades, cardiac surgical operations have become routine procedures, but the risk of perioperative complications remains high. Pericardial tamponade (PT) is a medical emergency leading to hypoperfusion of sensitive organs and, if untreated, cardiogenic shock with circulatory collapse. The routine use of extracorporeal circulation (ECC) in cardiac surgical interventions requiring cardiopulmonary bypass (CPB) by itself poses a non-negligible risk of systemic inflammatory response and organ damage.

This thesis focusses on the design of clinically relevant large animal models of PT and CPB and the therapeutic application of methane (CH_4) in PT- and CPB-induced splanchnic and renal changes, especially on the modulation of inflammatory pathways. We designed and conducted two series of experimental studies to investigate whether CH_4 has an effect on sensitive organs in PT-induced cardiogenic shock or CPB-induced systemic inflammatory response.

In *Study I,* we performed experiments on three groups of minipigs. Group 1 served as the sham-operated control; in Groups 2 and 3, surgical PT was induced for 60 min with a novel technique with trans-phrenic pericardial cannula insertion. Group 3 was treated with 2.5% v/v normoxic CH_4 through the ventilator. Haemodynamics and mesenteric macro- and microcirculation were monitored, the components of mucosal inflammatory response, intestinal mast cell activation and leukocyte function were detected in tissue samples, and superoxide content was measured in whole blood samples. Inhalation of CH_4 had no impact on the macrohaemodynamic status of the animals after the release of PT, but mucosal microcirculation and *in vivo* histology data showed significant improvement. In line with these findings, both leukocyte accumulation and mast cell degranulation decreased, and the superoxide amount of whole blood was lowered in the CH_4-treated group.

In *Study II*, we designed and employed an experimental model of CPB using anaesthetized minipigs in two groups. Groups 1 and 2 both underwent 60 minutes of centrally cannulated CPB. Group 2 received 2.5% v/v normoxic CH_4 added to the oxygenator sweep gas. Renal artery (RA) flow was monitored, and hourly diuresis was measured. Activities of xanthine oxidoreductase (XOR) and myeloperoxidase (MPO) were determined from cardiac, intestinal and renal tissue samples. Superoxide content was measured in whole blood samples. CH_4 administration improved the severe impairment of RA flow and maintained the hourly diuresis in the recovery period after ECC. XOR, a significant source of superoxide, was present with significantly lower

activity in cardiac, small intestinal and renal tissue samples. In line with these findings, lower superoxide levels and reduced intestinal MPO activities were found, and the inotropic demand was also lower in CH_4-treated animals.

Overall, the evidence suggests that the application of CH_4 in these porcine models of cardiac surgery can effectively reduce organ damage by influencing XOR-dependent ROS production, and leukocyte and mast cell activation. These results suggest that exogenous CH_4 may be a novel, additional therapeutic option to reduce the risk of perioperative cardiac surgical inflammatory reactions.

TABLE OF CONTENTS

1. INTRODUCTION

1.1. Biological gases and gasotransmitters

Many gases in the Earth's atmosphere, such as oxygen (O_2) and carbon dioxide (CO_2), are physiologically important or biologically irreplaceable. A number of other gases that occur naturally, such as nitric oxide (NO), carbon monoxide (CO) and hydrogen sulphide (H_2S), are considered "gasotransmitters", with diverse effects on the basal functions of aerobic cells. According to current views, a member of this category of gas must adhere to four characteristics (simplicity, availability, volatility and effectiveness) and meet six criteria: (a) small molecules, (b) freely permeable to membranes, (c) endogenously generated in mammalian cells with specific substrates and enzymes, (d) serve well-defined specific functions at physiologically relevant concentrations, (e) functions can be mimicked by their exogenously applied counterparts, and (f) have specific cellular and molecular targets (1). In general, gasotransmitters play vital regulatory roles in maintaining homeostasis in the human body through distinct biochemical pathways.

1.2. Methane

Methane (CH_4) is also part of the gaseous environment which maintains the aerobic metabolism, but its role in cellular physiology is largely unmapped, and relevant data on human cardiovascular effects is sparse. It is an inert, colourless, odourless organic molecule, the main component of natural gas, with low solubility in water (0.02 g/kg of water at 22°C room temperature). It is a simple asphyxiant, which means that tissue hypoxia might occur when an increasing concentration of CH_4 displaces inhaled air in a restricted area. In the atmosphere – which currently contains approximately 1.7–2.0 ppmv (parts per million by volume) – CH_4 is an important greenhouse gas.

1.3. Abiotic and biotic methane generation

There are two main forms of methanogenesis, abiotic and biotic generation. Abiotic CH_4 formation is mainly associated with emissions from mining and combustion of fossil fuels, and the burning of biomass, where CH_4 formation is possible at high temperatures and/or elevated pressures, which are irrelevant in biological environments (2). Biotic CH_4 formation takes place through anaerobic fermentation by a unique class of prokaryotes (archaea) in ruminants or other mammals or in the environment, where organic matter decomposes in the absence of oxygen or other

oxidants. The predominant methanogenic archaeon in the human large intestine is *Methanobrevibacter smithii* (3), and the catalyzing enzyme of this pathway is methyl co-enzyme M reductase, with the use of CO_2 and H_2 as main substrates (1).

In contrast to ruminants, which all emit substantial amounts of CH_4, only around one third of humans are considered to be CH_4 producers. In humans, CH_4 producers and CH_4 non-producers are distinguished clinically by breath analysis, where production is defined as an increase of more than 1 ppm above the atmospheric level in the exhaled air (4). However, it has been shown recently by precise measurement techniques that CH_4 production can be detected in all individuals (5), although in quite a wide range of magnitude and dynamics; therefore, there seems to be a discrepancy between older data and the latest. In addition, there is an ongoing debate whether CH_4 production is genetically or environmentally determined or whether it is a result of yet unknown factors. Indeed, other studies have confirmed direct CH_4 release from eukaryotes, including plants and animals, in the absence of microbes and in the presence of oxygen (6–8). Further, several data have established the possibility of biotic, non-archaeal CH_4 generation in eukaryotic cells under various conditions involving mitochondrial dysfunction (4). In summary, the overall evidence suggests that the excretion of CH_4 in the breath of mammals reflects not only intestinal microbial fermentation, but also unidentified generation from target cells (9).

1.4. Bioactivity of exogenous CH_4 – anti-inflammatory effects

The current evidence does not fully support the gasotransmitter concept, but it does support the notion that CH_4 is bioactive. Although CH_4 is widely regarded as inactive, a number of studies have demonstrated explicit biological effects in living biological systems (10). An anti-inflammatory potential for CH_4 was first reported in a canine model of intestinal ischaemia-reperfusion (I-R) (11), and thereafter other reports have confirmed the antioxidant and anti-apoptotic effects of exogenous CH_4 administration in various *in vitro* and *in vivo* settings (12–21). The exact mechanism of action is not fully clarified, but it has been shown that the anti-inflammatory action is mediated through the inhibition of polymorphonuclear (PMN) leukocyte activation and reduced reactive oxygen species (ROS) production (11). Other experimental data have also shown that the biological effects are related to the inhibition of xanthine oxidoreductase (XOR) activity as well, thus lowering the amount of superoxide radical formation (22). Superoxide is one of the most important reactive oxygen species (ROS) and a potent activator of effector cells like polymorphonuclear (PMN) leukocytes and

mast cells in the small intestine. In this line, a previous study has demonstrated that exogenous CH_4 inhalation was protective in I-R-induced nitrergic neuronal changes and inhibited XOR-linked reactions during hypoxia-mediated intestinal injury (22). Other findings provided evidence that administration of CH_4-enriched saline solutions is protective in experimental liver failure (12), autoimmune hepatitis (23), acute lung injury (15), and hepatic (13), spinal cord (15), retinal (16), myocardial (17) and skin I-R injuries (18). Today the overall evidence points to the likelihood that exogenous CH_4 can influence different intracellular signalling pathways, which may be therapeutically exploited to attenuate the signs and consequences of inflammation (24).

1.5. The inflammatory consequences of low cardiac output states

Perioperative local and/or systemic inflammation due to the natural aetiology of cardiac diseases and/or the invasive nature of technical interventions represents a major correlative risk of cardiac surgery and a key component of postoperative complications. Maintaining cardiac function is essential in keeping the distal perfusion of organs before, throughout and after the surgical procedure. Low cardiac output (CO) states, such as pericardial tamponade (PT), post-cardiotomy cardiac stunning and perioperative myocardial infarction, often lead to cardiogenic shock, with a high risk of morbidity and mortality. Nevertheless, permanently low CO, even without definite signs of cardiogenic shock, can induce microcirculatory impairment in peripheral tissues, triggering local and later systemic inflammatory responses. In this respect, early measures of management are clearly needed to avoid permanent organ failure or death (25).

Furthermore, reperfusion, i.e. the restoration of blood flow after a period of ischaemia, can also place previously ischaemic organs at risk of further cellular necrosis and limited recovery (26). This phenomenon is termed I-R injury. Reperfusion injury is mainly mediated by ROS formation in the re-oxygenized tissues, and the main source in the intestines is xanthine oxidoreductase (XOR) and accumulated PMNs, a second wave cellular response of critical importance in mucosal I-R damage. The process is often associated with microvascular injury and the dysfunction of the endothelium, leading to increased permeability of capillaries, damage to plasma membranes, proteins and DNA in the cells (27).

1.6. Pericardial tamponade

Among the major complications of cardiac surgical interventions, PT is considered as one of the most dramatic pathological conditions affecting both the macro- and microhaemodynamics of the human body. The lack of urgent treatment can lead to cardiogenic shock and is inevitably followed by multi-organ failure and death (28). PT is caused by fluid accumulation within the pericardial sac. Transudation can be a consequence of severe renal failure, neoplastic diseases or end-stage heart failure (29). Inflammatory diseases with various aetiologies can lead to massive pericarditis and purulent pericardial effusions. However, PT can most likely be an early or late haemorrhagic complication of acute type-A aortic dissection, chest trauma, or cardiac surgical procedure or intervention. The mortality rate is usually very high, but due to the large aetiological variability, exact statistical data are rarely available; thus, comparisons between different pathologies are pointless. In a high volume patient care centre, the all-cause in-hospital mortality was shown to be approx. 20% and the 30-day mortality ranged from 25 to 35% (30). The rate of fluid accumulation within the pericardial sac determines the haemodynamic effects and the clinical picture as well. The 2015 ESC clinical guidelines on the management of pericardial diseases propose an echocardiographic (ECHO) classification based on the largest ECHO-free space and step-by-step scoring system-based management (31). Nevertheless, understanding the exact pathophysiologic mechanisms of PT is the key to taking the necessary diagnostic steps and to choosing the optimal therapeutic options for patients.

Acute PT is a rapidly progressive condition, in which there is usually no time for slower compensatory mechanisms to develop. It has been shown that strong sympathetic neurohormonal activation evolves and that the release of endogenous vasopressors is also significant (32). Peripheral vasoconstriction elevates the afterload, which can worsen distal organ hypoperfusion and increases the myocardial oxygen demand by elevating left ventricular workload. When the acute compensatory responses are depleted, rapid circulatory collapse develops.

1.7. ECC-induced systemic inflammation in cardiac surgery

Since the first successful open-heart surgery with cardiopulmonary bypass (CPB) by John Gibbon on May 6, 1953, thousands of such procedures have been carried out worldwide each year. However, despite the safety of modern CPB circuits, extracorporeal circulation (ECC) is still associated with some degree of post-operative inflammatory activation, similar to the septic systemic inflammatory response (SIRS).

It is generally triggered immediately during CPB, and if the circulatory support is prolonged, e.g. during a complex operation requiring deep hypothermic circulatory arrest, the degree of inflammatory response can be much higher with higher risk for multi-system organ failures. Indeed, besides cardiogenic shock-induced I-R damage, the ECC or other means of ECC, such as extracorporeal membrane oxygenation (ECMO), can themselves contribute significantly to the evolution of SIRS after cardiac surgery (33,34).

It has been shown that blood contact with the foreign surface of the CPB circuit activates humoral and cellular factors (34), leading to the intrinsic activation of the coagulation cascade. Due to the routine use of heparin before initiation of ECC, thrombin and fibrin complexes are not formed, but the first steps of the coagulation cascade are activated along with other pro-inflammatory cascades, such as the kinin–kallikrein system or the complement system, triggering a wide variety of cellular systems, such as endothelial cells, leukocytes, thrombocytes and mast cells (33). If these cascade activations are dysregulated due to prolonged CPB time or metabolic changes, significant tissue and organ damage can occur in sensitive organs such as the kidneys and intestines. Therefore, a search for novel therapeutic strategies to reduce post-CPB inflammatory damage is an important clinical and scientific research goal.

1.8. Hypoperfusion-induced intestinal damage

Among the organs affected by cardiogenic shock, the gut plays an important role in preserving a solid barrier between the bloodstream and the outside world. It is of vital importance to preserve the endothelial and epithelial functions of the mucosa to prevent bacterial translocation and thus sepsis. Low CO states like PT have a strong impact on mesenteric circulation by triggering local splanchnic hypoxia due to endogenous vasoconstriction. A diverse system of cascades, including pro-inflammatory cytokines and complement factors, enhances mucosal leukocyte recruitment and amplifies the local inflammatory response. Among the numerous vasoconstrictors, the endothelin-1 (ET-1) system plays a pronounced role in the maintenance of splanchnic hypoxia, mucosal leukocyte accumulation and triggering mast cell degranulation as well (35).

1.8.1. Mast cell-associated mucosal injury

The mucosal damage induced by low CO states is largely dependent on local vasoactive responses which influence various secondary cellular mechanisms. Mast

cells are key participants in these responses (36)(37). These multifunctional cell populations play various roles in the homeostatic stability of the connective tissue, and are key elements in local vasoregulation. Mast cells are oval-shaped 4–24 μm cells, morphologically similar to basophil leukocytes with about 40% of their cytoplasm containing secretory granules (38). The main sub-populations can be classified according to the anatomical position or the biochemical patterns defined by the granule composition. Traditionally, Mucosal Mast Cells (MMCs) and Connective Tissue Mast Cells (CTMCs) are distinguished based on their histochemical staining properties (39). Both populations are present around capillaries or neurons, mainly in anatomical locations which are close to barriers to the surrounding world, such as the skin, the lungs and the mucosa in the digestive system. MMCs are mainly present in the sub-mucosal layer in close proximity to postcapillary venules in the stomach, and small and large intestines, and contain tryptase, a serine protease as active secretory ingredient. CTMCs are mainly present in the connective tissue in the skin and contain chymase, tryptase and carboxypeptidases (40). According to their anatomic position, MMCs can respond to stimuli and outside effects induced by antigens, bacteria, viruses and fungi by degranulation of preformed cytoplasmic vesicles, thus influencing the vasoactive responses (41). In addition, mast cells can also generate and actively secrete de novo formed mediators (cytokines and growth factors) and mediate the mobilization of other inflammatory effector cells.

Among the biogenic mediators, MMCs contain histamine, serotonin and dopamine; degranulation thus leads to vasodilation and oedema formation through increased capillary permeability (32-34). Preformed cytokines like interleukin-4 (Il-4), Il-5, tumour necrosis factor (TNF) and chemokines can bring about leukocyte adhesion and extravasation, thus augmenting the immune response. In the case of ongoing inflammation, both leukocytes and MMCs will mediate and amplify tissue injury with the release of proteases, such as chymase, tryptase, matrix metalloproteinases (MMPs), and ROS formation (40,43–45).

The activation and degranulation of MMCs can proceed through two main pathways. The immune pathway is immunoglobulin E (IgE)-mediated and high-affinity IgE receptor (FcεRI)-linked and is a possible contributor to intestinal allergic diseases (41). There is conflicting data on the non-immunologic activation pathways, but it is likely that G protein-coupled receptor activation and intracellular pathways triggered by MMC-produced substances play a vital role in I-R-derived MMC activation (46,47).

These involve endothelin (35), complement (48) and adenosine receptor (49)-linked activation. It is also known that ROS is an important component of the biochemical pathway in MMC degranulation, and in fact inhibition of ROS formation can prevent degranulation (45).

1.8.2. Leukocyte recruitment and ROS production

To date much progress has been made in understanding the different biochemical pathways which lead to I-R damage (26). Leukocyte recruitment after intestinal I-R is a multi-pathway process with the involvement of cellular interactions and chemotactic signals. The primary site of leukocyte migration is across the endothelial wall of post-capillary venules. Each endothelial tissue has a specific pattern of anchoring transmembrane glycoproteins, such as P- and E-selectins from the selectin family, α_4- and β_2-integrins, and intercellular adhesion molecule 1 (ICAM-1) for leukocyte capturing, binding and activation (44). The dynamics of inflammation are thus unique for every tissue. This is also true for the expression of chemotactic patterns (IL-1,-3,-6,-8 and TNF) (50)(38) by the cells involved in immunomodulation, most importantly mast cells, endothelial cells and leukocytes.

Reperfusion-mediated ROS production is a significant contributor to ischaemic mucosal damage. ROS formation can occur in the mitochondria throughout the hypoxic phase and after reperfusion as well, but the key ROS producer is most probably intestinal XOR (51), which is present in high concentration in many species, including humans. In normoxic states, xanthine dehydrogenase (XDH - EC 1.17.1.4) is a key enzyme in purine catabolism, which converts xanthine to urate with nicotinamide adenine dinucleotide (NAD^+) and H_2O as a proton acceptor (52). In hypoxic conditions, however, the enzyme is reversibly or irreversibly converted to xanthine oxidase (XO) form (EC 1.17.3.2). During reperfusion, XO will catalyse the conversion of 1 mol hypoxanthine to xanthine and to uric acid formation with the production of 2 mol superoxide (O_2^{-}), which will act as a substrate for other ROS and nitrosative radical species formation, a key factor in tissue leukocyte recruitment (53).

1.9. Hypoperfusion-induced kidney damage

CPB often affects the renal function of patients undergoing cardiac surgery, and acute kidney injury (AKI) is one of the most frequent complications of these procedures. The pathogenesis of the syndrome is complex and influenced by many factors, but it has been established that perioperative low CO or hypoperfusion in association with cardiogenic shock or hypovolemia can play critical pathogenic roles in the development and progression of AKI. Nevertheless, the exact molecular pathomechanism is still unclear, and it has been suggested that further research should be focussed on the investigation of novel supportive therapies and the development of new pharmacological approaches aimed at reducing AKI occurrence. In this line, there is evidence that the activation of the ET-1 system may be a potent mediator of vasoconstriction, inflammation and oxidative stress reaction that could lead to AKI. It has been demonstrated that the administration of ET-A receptor antagonist compound reduced the number of inflammatory cells and improved kidney function as well in a pig model of post-CPB kidney injury (54).

1.10. *In vivo* models of PT- and CBP-induced SIRS

1.10.1. Animal models of PT

In a seminal paper, Lluch et al. described a canine model of cardiogenic shock, where the left ventricular function was reduced by coronary embolization (55). Since then, numerous refinements have been made to study the immediate and late macro- and microhaemodynamic consequences, but a reproducible, well-controlled and stable experimental setting is still needed. The *in vivo* reduction of myocardial function can be carried out relatively easily by selective coronary ligation or embolization, but the technique is accompanied by high mortality due to malignant arrhythmias. On the other hand, it is possible to reduce cardiac output by obstructing ventricular filling and lowering the left ventricular stroke volume, a condition that can be achieved by inducing PT. Our research group has previously demonstrated that PT is indeed an appropriate model to study the pathomechanism of cardiogenic shock (32). These experiments were carried out on anaesthetized, mechanically ventilated dogs, and it has been shown that peripheral haemodynamics and vasoactive humoral responses could be monitored in sufficient detail (32). In this setup, PT is induced by infusion of saline through a cannula placed in the pericardium via thoracotomy, and the progression could be immediately terminated by fluid extraction from the pericardium. This has thus become a standard model for studying the consequences of reversible cardiogenic

shock (56). The inherent disadvantage of the model is thoracotomy itself and the possibility of impaired lung function.

1.10.2. Animal models of extracorporeal circulation

The technological development of human ECC devices capable of providing sufficient perfusion was based on a variety of *in vivo* experiments and animal trials. Since then, many refinements have been made to perfect the CBP technique for clinical use; however, basic problems, such as inflammatory reactions and cellular damage to circulating blood, have yet to be solved. Besides the technological needs of ECC circuit development, the basic pathophysiological problems require the use of well-established, stable animal models. Due to the high costs of CBP components and supplemental expenses, *in vivo* ECC studies are performed in only few research institutions. Swine, dogs, cows and sheep are usually employed as models (57), but the general disadvantage of heavy equipment use and the requirement of a full-scale operative environment remain. It would be possible to perform small animal experiments, using rodents (58), to reduce costs, time and the need for manpower, but there are many other disadvantages, including species differences and the operative challenges in such small scales. In this sense, the porcine model of CPB is still considered the best platform for the translational development of novel organ protection strategies.

2. MAIN GOALS

Cardiac surgery-related perioperative inflammatory activation is a significant clinical problem, and there is a clear need for efficient adjuvant therapies to influence the outcome of such events. Our first aim was to develop and design suitable *in vivo* models, where the characteristics of the postoperative clinical syndrome can be examined under standardized conditions.

1. A main disadvantage of the currently used large animal PT models is thoracotomy itself with impaired lung function and extended wound surface with a high risk of bleeding complication, and lung and tissue injury. Our aim was to design an experimental procedure to model iatrogenic PT, where thoracotomy can be avoided, but the situation is realistic, similar to the clinical appearance.

2. Secondly, we aimed to characterize the ECC-induced haemodynamic and microcirculatory consequences in a clinically relevant larger animal model with anatomical and immunological similarities to humans.

In these experimental protocols, we placed special emphasis on identifying the characteristic haemodynamic and microcirculatory changes and main components of the peripheral inflammatory response, including signs of mucosal mast cell and leukocyte activation. Thereafter, the main purpose of our succeeding studies was to verify and characterize the effects of exogenous CH_4 administration in these model scenarios.

3. Previous evidence demonstrated the anti-inflammatory capacity of CH_4 with the possibility of modulating the pathways leading to oxidative stress. Therefore, our next aim was to outline the intestinal effects of CH_4 inhalation in a standardized large animal model of experimental PT. For this purpose, normoxic CH_4 was administered through the ventilator of anaesthetized minipigs during PT-induced non-occlusive splanchnic I-R.

4. We also aimed to investigate whether the systemic inflammatory response caused by ECC could be modified with exogenous CH_4. The additional aim of this study was to determine whether CH_4 administration would influence the development of post-CPB kidney dysfunction. We investigated this hypothesis in anaesthetized minipigs with centrally cannulated ECC with normoxic CH_4 added to the oxygenator gas sweep.

3. MATERIALS AND METHODS

3.1. Experimental animals

The experiments were performed in accordance with National Institutes of Health guidelines on the handling and care of experimental animals and EU Directive 2010/63 on the protection of animals used for scientific purposes. The studies were approved by the Animal Welfare Committee of the University of Szeged (approval number: V/148/2013).

3.2. Animals and anaesthesia

28 male outbred Vietnamese minipigs (weighing 45±8 kg) were used (n=18 in *Study I*, n=10 in *Study II*). A mixture of ketamine (20 mg kg^{-1}; CP-Ketamin 10%; Pordulab Pharma-induced anaesthesia. Raamsdonksveer, Netherlands) and azaperone (2 mg kg^{-1}; Stresnil; Elanco Animal Health, Vienna, Austria) was administered intramuscularly. After endotracheal intubation, mechanical ventilation was started with a tidal volume of 10 ml kg^{-1}, and the respiratory rate was adjusted to maintain the end-tidal pressure of CO_2 and partial pressure of CO_2 in the 35–45 mmHg ranges. Anaesthesia was maintained with a continuous infusion of propofol (50 µl $min^{-1}kg^{-1}$ *iv*; 6 mg $kg^{-1}h^{-1}$; Propofol; Fresenius Kabi, Bad Homburg, Germany), midazolam (1.2 mg $kg^{-1}h^{-1}$; Midazolam Torrex; Torrex Chiesi Pharma, Vienna, Austria) and fentanyl (0.02 mg $kg^{-1}h^{-1}$; Fentanyl-Richter; Richter Gedeon, Budapest, Hungary), while muscle relaxation was maintained with pipecuronium (single administration, 4 mg dose; Arduan; Richter Gedeon, Budapest, Hungary).

3.3. Surgical interventions, Study I (Aims 1 and 3)

The left jugular vein was cannulated for fluid and drug administration. The left femoral artery was cannulated for the measurement of mean arterial pressure (MAP), heart rate (HR) and CO by transpulmonary thermodilution (PiCCO Catheters; PULSION Medical Systems, Feldkirchen, Germany). MAP, HR and CO data were recorded, while pressure signals (BPR-02 transducer; Experimetria Ltd, Budapest, Hungary) and superior mesenteric artery (SMA) flow signals (T206 Animal Research Flowmeter; Transonic Systems Inc., Ithaca, NY, USA) were measured continuously and registered with a computerized data-acquisition system. Urine output was assessed by surgically placing a urinary catheter in the bladder via the femoral incision. The urine was collected and measured at the end of the observation period to calculate average hourly diuresis. Ringer's lactate was given at a rate of 10 $mlkg^{-1}h^{-1}$. After a

median laparotomy, a flow probe was placed around the SMA (Transonic Systems Inc., Ithaca, NY, USA). The wound in the abdominal wall was temporarily closed thereafter with clips. In addition, intravital examination of intestinal microcirculation was carried out with an orthogonal polarization spectral imaging system (OPS; Cytoscan A/R, Cytometrics, Philadelphia, PA, USA), and the extent of damage to the gastric mucosa was evaluated by *in vivo* histology (Five1, Optiscan Pty. Ltd., Melbourne, Victoria, Australia). The diaphragm was accessed through a median laparotomy. A 3-cm incision was made at the sternal part, avoiding the muscular region of the diaphragm. The pericardium was opened, and a cannula was fixed into the pericardial cavity with a pledgeted purse-string suture (Figure 1). The tamponade was induced and maintained for 60 min by intrapericardial administration of heparinized own blood (100±50 ml), and MAP was maintained at 40–45 mmHg. The abdominal wall was closed with surgical clips during the observation period and between microcirculatory image recordings.

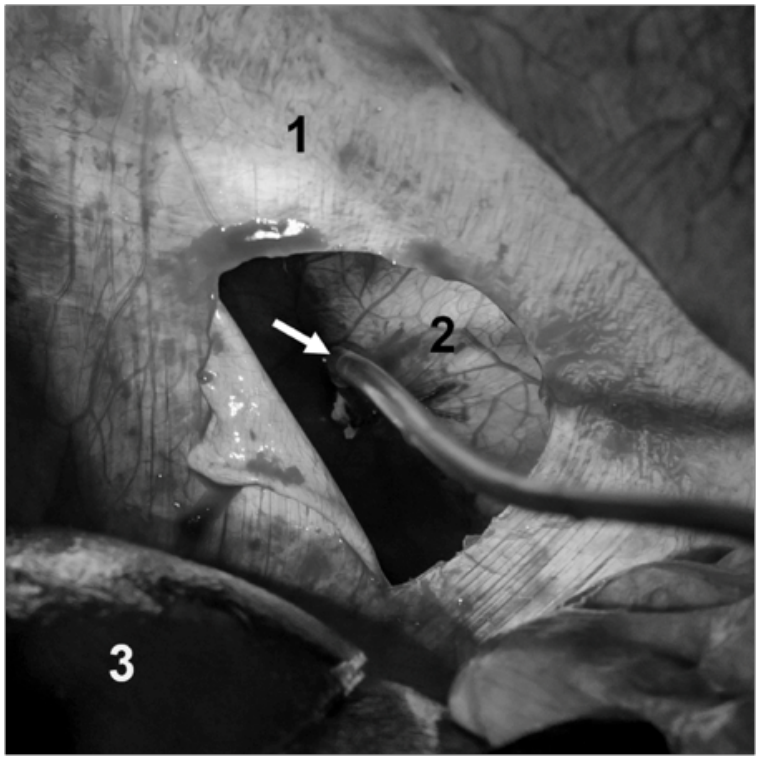

Figure 1. *The insertion of the pericardial cannula via the transphrenic route (**1** diaphragm, **2** pericardium, **3** liver, **arrow:** the cannula fixed into the pericardium).*

3.4. Surgical interventions, Study II (Aims 2 and 4)

The anaesthetized animals were placed in a supine position on a heating pad to maintain body temperature between 36 and 37°C and received an infusion of Ringer's lactate solution at a rate of 10 ml kg^{-1} hr^{-1} during the experiments. The left jugular vein was cannulated for fluid and drug administration, and the left femoral artery was also cannulated to measure MAP, HR and CO by transpulmonary thermodilution. After a median laparotomy, the renal artery (RA) was dissected free, and a flow probe was placed around the blood vessel (Transonic Systems Inc., Ithaca, NY, USA) to measure blood flow. The abdominal incision was temporarily closed with clips. A urinary catheter was surgically placed in the bladder via the femoral incision. The urine was collected and measured at the end of the observation period to calculate average hourly diuresis.

A median sternotomy was performed and the pericardium dissected. The aorta was dissected free and circled with tape. After the administration of heparin (Heparibene; Teva, Budapest, Hungary) (2000 IU iv) and activated clotting time (ACT) control (ACT > 500 sec), purse-string sutures were placed in the ascending aorta and the right atrial appendage, and standard central CPB cannulation was performed (Figures 2 and 3). Due to the lack of aortic cross clamping and the fragility of the upper pulmonary vein, venting was not used. Cardiotomy suction was not employed because the aorta or the cardiac chambers were not open. After the baseline haemodynamic measurements, CPB was initiated and respiration stopped. CPB was carried out with a modular perfusion system (Therumo Sarns 8000; Terumo Cardiovascular, Ann Arbor, MI, USA) using a disposable hollow fibre oxygenator (CAPIOX®; Terumo Cardiovascular, Ann Arbor, MI, USA). In addition, the cessation of the respiration achieved maximal peak blood and cellular CH_4 concentration in the treated animals. The Du Bois formula was applied for non-invasive estimation of the CO to calculate the body surface area, and 2.4 l/m^2 CI was used standardly for all the animals. After the insertion of the central venous line and the PiCCO cannula in the femoral artery, CO was measured directly with the PiCCO system via thermodilution. The measured and estimated CO values were nearly identical in all cases. Oxygenator gas sweeps were adjusted to post-membrane arterial blood gas samples.

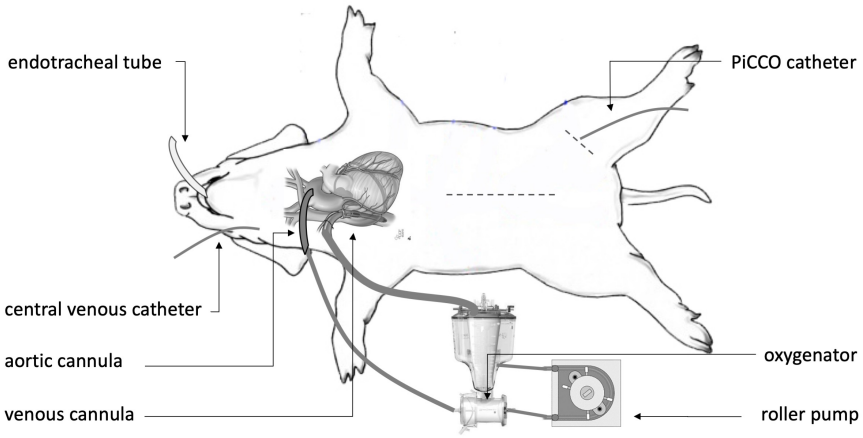

Figure 2. *Schematic illustration of the surgical setting of CPB in Study II.*

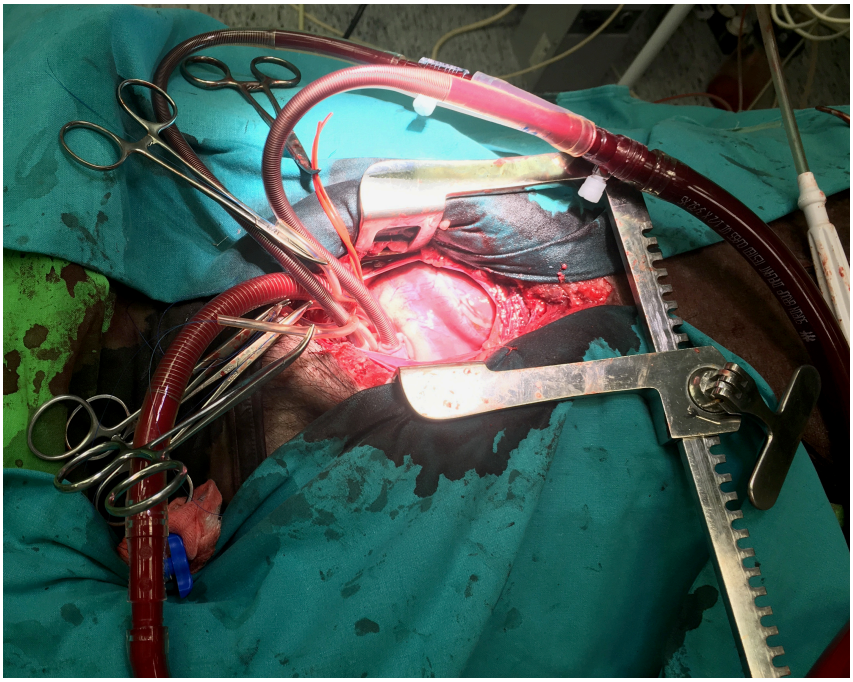

Figure 3. *The central cannulation of CPB in Study II.*

3.5. Measurements

3.5.1. Haemodynamic measurements

MAP, CO and HR were monitored with the PiCCO Plus monitoring system (PULSION Medical Systems; Munich, Germany). Blood flow signals (T206 Animal Research Flowmeter; Transonic Systems Inc., Ithaca, NY, USA) were recorded and registered with a computerized data acquisition system (SPELL Haemosys; Experimetria, Budapest, Hungary).

3.5.2. Measurement of blood CH_4 content

A near-infrared laser technique-based photoacoustic spectroscopy apparatus (60) was employed to confirm the presence of exogenous CH_4 in the blood. Blood samples were taken from the aorta and jugular vein (5 ml from each) and placed in a glass vial with 20 ml headspace volume and closed so as to be airtight. The outlet of the vials was connected to the spectroscope pump, headspace gas was pumped into the chamber of the device at a rate of 10 mL/min, and the CH_4 content of the air above the blood samples was measured. The CH_4 values were corrected for background levels and expressed in ppm.

3.5.3. Tissue harvesting and processing

Tissue biopsies kept on ice were homogenized in a phosphate buffer (pH 7.4) containing 50 mM Tris-HCl (Reanal, Budapest, Hungary), 0.1 mM EDTA, 0.5 mM dithiothreitol, 1 mM phenylmethylsulfonyl fluoride, 10 μg ml^{-1} soybean trypsin inhibitor and 10 μg ml^{-1} leupeptin (Sigma-Aldrich GmbH, Germany). The homogenate was centrifuged at 4°C for 20 min at 24 000 g, and the supernatant was loaded into centrifugal concentrator tubes (Amicon Centricon-100; 100 000 MW cut-off ultrafilter). XOR activity was determined in the ultrafiltered supernatant, while that of MPO was measured on the pellet of the homogenate.

3.5.4. Histology for light microscopy of leukocytes and mast cells

Full-thickness ileal biopsies taken at the end of the experiments were analysed in each group. The tissue was fixed in 6% buffered formalin, embedded in paraffin, cut into 4-μm-thick sections and stained with haematoxylin and eosin. The infiltration of leukocytes was detected and the number of leukocytes counted in at least 20 fields of view at an original magnification of 400x.

Intestinal biopsy samples for light microscopy were rapidly placed into ice-cold Carnoy's fixative and trimmed along the longitudinal axis. The fixed tissue was attached to a hard cardboard backing to ensure the optimal longitudinal direction of the section. The samples were embedded in paraffin, sectioned and stained with haematoxylin-eosin, acidic toluidine blue (pH 0.5) or alcian blue-safranin O (pH 0.4). MCs stained positively were quantitated in the villi of an average of 20 villus-crypt units. The counting was performed in coded sections at 400 optical magnifications by one investigator. Loss of intracellular granules and stained material dispersed diffusely within the lamina propria were taken as evidence of mast cell degranulation.

3.5.5. Tissue MPO activity

Being a marker of tissue leukocyte infiltration, MPO activity was measured on the pellet of the homogenate (61). Briefly, the pellet was resuspended in a K_3PO_4 buffer (0.05 M; pH 6.0) containing 0.5% hexa-1,6-bis-decyltriethylammonium bromide. After three repeated freeze-thaw procedures, the material was centrifuged at 4°C for 20 min at 24 000 g, and the supernatant was used for MPO determination. Next, 0.15 ml of 3,3',5,5'-tetramethylbenzidine (dissolved in DMSO; 1.6 mM) and 0.75 ml of hydrogen peroxide (dissolved in K_3PO_4 buffer; 0.6 mM) were added to 0.1 ml of the sample. The reaction led to the hydrogen peroxide-dependent oxidation of tetramethylbenzidine, which could be detected spectrophotometrically at 450 nm (UV-1601 spectrophotometer; Shimadzu, Kyoto, Japan). MPO activities were measured at 37°C; then the reaction was halted after 5 min with the addition of 0.2 ml of H_2SO_4 (2 M). The data were expressed in terms of protein content.

3.5.6. XOR activity

XOR activity was determined in the ultrafiltered, concentrated supernatant with a fluorometric kinetic assay based on the conversion of pterine to isoxanthopterine in the presence (total XOR) or absence (XO activity) of the electron acceptor methylene blue (62).

3.5.7. Whole blood superoxide production

The chemiluminometric method developed by Zimmermann et al. (63) was used for the whole blood superoxide production measurements. During the measurements, 10 µl of whole blood was added to 1 ml of Hank's solution (PAA Cell Culture, Westborough, MA, USA), and the mixture was maintained at 37°C until assay. The chemiluminometric response was measured with a Lumat LB9507 luminometer

(Berthold, Wildbad, Germany) during a 30 min period after the addition of 100 µl of lucigenin.

3.5.8. Microcirculatory measurements

An intravital orthogonal polarization spectral imaging technique (Cytoscan A/R; Cytometrics, Philadelphia, PA) was used for non-invasive visualization of the mucosal microcirculation of ileum. This technique utilizes reflected polarized light at the wavelength of the isosbestic point of oxy- and deoxyhaemoglobin (548 nm). As polarization is preserved in reflection, only photons scattered from a depth of 200 to 300 µm contribute to image formation. A ×10 objective was placed onto the mucosal surface of the small intestine, and microscopic images were recorded with a S-VHS video recorder 1 (Panasonic AG-TL 700; Matsushita Electric, Osaka, Japan). Quantitative assessment of the microcirculatory parameters was accomplished offline with a frame-to-frame analysis of the videotaped images. Red blood cell velocity (RBCV, µm/s) changes in the capillary were determined in three separate fields by means of a computer-assisted image analysis system (IVM Pictron, Budapest, Hungary). The same investigators performed all the microcirculatory evaluations.

3.5.9. *In vivo* detection of mucosal damage

The extent of damage to the ileal mucosa was evaluated by means of fluorescence confocal laser scanning endomicroscopy (CLSEM) developed for *in vivo* histology. Two investigators performed the analysis twice, separately. The mucosal surface of the ileum was surgically exposed and laid flat for examination. The ileal mucosal structure was recorded after the topical application of the fluorescent dye acriflavine (Sigma-Aldrich Inc., St. Louis, MO, USA). The surplus dye was washed off with saline 2 min before imaging. The objective of the device was placed onto the mucosa, and confocal imaging was performed 5 min after dye administration (1 scan/image, 1024 x 512 pixels and 475 x 475 µm per image). The changes in the mucosal architecture were examined with a semi-quantitative scoring system as described previously (64). Briefly, (I) oedema (0 = no oedema, 1 = moderate epithelial swelling, 2 = severe oedema) and (II) epithelial cell outlines (0 = normal, clearly, well-defined outlines, 1 = blurred outlines, 2 = lack of normal cellular contours).

3.6. Experimental protocols

3.6.1. Experimental protocol in Study I

The animals were randomly allocated into three experimental groups (Figure 4). Group 1 (n=6) served as a sham-operated control, with the same surgical interventions, time frame and sampling as in Group 2 (n=6) but without the induction of PT. Group 3 received inhaled 2.5% v/v normoxic CH_4 (Linde Gas, Hungary) in the last 5 minutes of PT and for an additional 10 min after PT. In Groups 2 and 3, after the end of 60-min PT, the blood was released from the pericardial sac and the animals were monitored for 180 min. Blood gases and haemodynamic parameters were measured every 30 min. An *in vivo* histological examination on the ileal mucosa and detection of PMN leukocytes were performed at baseline, 30 min after the relief of PT (90 min) and at the end of the experiments (240 min). Tissue biopsies were harvested at the baseline, 30 min after the relief of PT (90 min) and at the end of the experiments (240 min). Blood samples were taken at the baseline 30 min after the relief of PT (90 min) and at the end of the experiments (240 min).

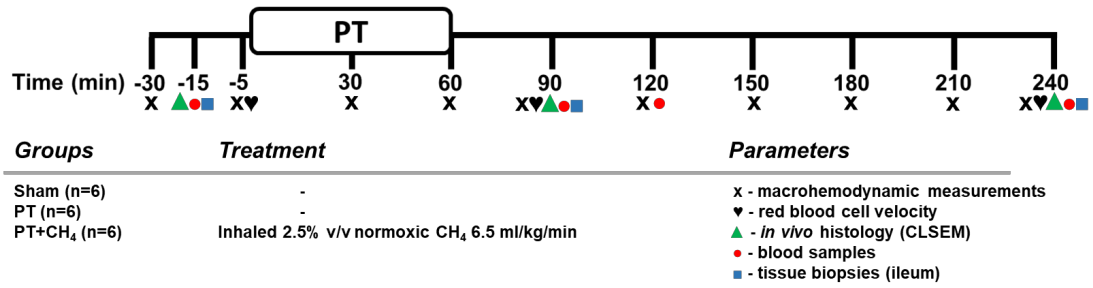

Figure 4. *The scheme of the experimental protocol for Study I.*

3.6.2. Experimental protocol in Study II

The animals (n=10) were randomly allocated into two experimental groups (n=5, each) (Figure 5). In both groups, CPB was maintained for 120 min and adjusted throughout according to the CO calculated for the animals. The heart was not cross-clamped nor arrested so as to exclude I-R and the accompanying inflammatory activation. Left heart venting was not used because the aorta was not cross-clamped, so the heart was left to beat and eject. After 120 min of CBP, flow was gradually decreased and stopped. The cannulas were removed, and the cannulation points were surgically closed. The non-treated CPB group (n=5) received a standard air–oxygen gas mixture with 0.6 FiO_2 at a flow rate of 2 l min^{-1} to the oxygenator. In the CH_4-treated

(CBP+Met) group, 2.5% v/v normoxic CH_4 (Linde Gas, Hungary) was added to the oxygenator gas sweep at a rate of 1 l min^{-1}. FiO_2 values were adjusted to the post-oxygenator PaO_2 values. The CH_4 content of the blood was monitored by near-infrared laser technique-based photoacoustic spectroscopy after 60 min of CH_4 treatment. The duration of CPB and the post-CPB times did not differ between the groups. The post-CPB haemodynamic stability (MAP > 60 mmHg) of the animal was maintained by continuous *iv* volume replacement (Ringer's lactate solution) and by maintaining the systemic vascular resistance with perfusion of norepinephrine if necessary (0.05–0.35 µg kg^{-1} h^{-1}; Arterenol; Sanofi-Aventis, Frankfurt am Main, Germany). After 120 min of post-CPB monitoring, a blood sample was taken to detect whole blood superoxide production, and small intestine, kidney and heart tissue biopsies were taken to measure MPO and XOR enzyme activity.

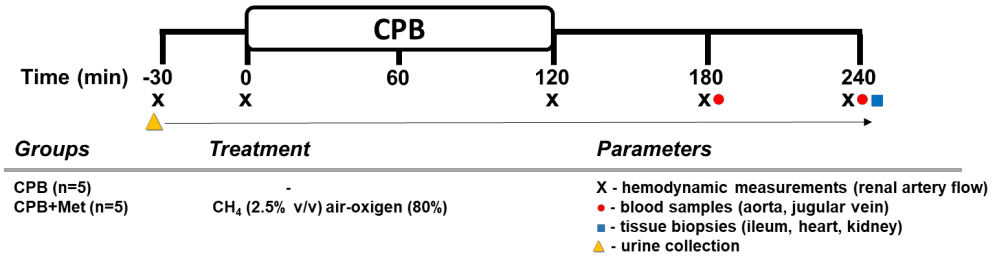

Figure 5. *The scheme of the experimental protocol for Study II.*

3.7. Statistical analysis

Data analysis was performed with a statistical software package (SigmaStat for Windows, Jandel Scientific, Erkrath, Germany). Friedman repeated measures analysis of variance on ranks was applied within groups. Time-dependent differences from the baseline for each group were assessed by Dunn's method. The differences between groups were analysed with the Mann–Whitney test. In the figures, median values and 75^{th} and 25^{th} percentiles are given; p values < 0.05 were considered significant.

4. RESULTS

4.1. Study I

4.1.1. Changes in haemodynamic parameters

The average duration of the surgical preparation phase was 70±20 min. MAP remained at 40–45 mmHg as previously planned throughout the 60 min of PT, accompanied by a concomitantly decreased CO and elevated HR (Table 1). After the release of PT, MAP started to increase. However, by the end of the observation period,

it was significantly lower compared to the baseline values and to the MAP for the sham-operated group. No significant difference was observed between the PT and PT + CH_4-treated groups. During the post-tamponade phase, the CO returned to the baseline values and there was no significant difference between the three groups. The same changes could be observed in the HR values (Table 1). The decreased venous return was evidenced by a significant elevation of CVP throughout the PT phase (data not shown). The SMA flow showed a significant drop in the PT phase as expected (Figure 6). After the release of PT, the SMA flow dramatically increased but did not reach the baseline values. Differences in SMA flow between CH_4-treated and non-treated groups were not observed.

Group	-5 min	60 min	120 min	180 min	240 min
			Cardiac index (L/min^{-1} m^{-2})		
Sham-operated	**2.6** *2.4; 2.7*	**2.4** *2.3; 2.6*	**2.3** *2.2; 2.5*	**2.4** *2.2; 2.8*	**2.4** *2.1; 2.7*
Cardiac tamponade	**2.5** *2.2; 3*	**1.2*^{x}** *1.2; 1.4*	**2.2** *1.9; 2.3*	**2.4** *2.2; 2.8*	**2.1** *2; 2.3*
Cardiac tamponade + methane	**2.4** *2.1; 2.9*	**1.1*^{x}** *1.1; 1.2*	**2** *1.9; 2.7*	**2.2** *2; 2.3*	**2.1** *1.9; 2.2*
			Mean arterial pressure (mmHg)		
Sham-operated	**93.4** *87.4; 104.3*	**101.6** *89.1; 111.3*	**100.9** *85.4; 112.1*	**93.3** *83.4; 98.6*	**94.3** *82.3; 101.5*
Cardiac tamponade	**95** *91; 101*	**43.1*^{x}** *39.5; 44*	**75** *68; 86*	**71*^{x}** *66.5; 77*	**72.5*^{x}** *63.5; 83*
Cardiac tamponade + methane	**98** *95.5; 104*	**46*^{x}** *45; 48.5*	**78.5** *69; 111*	**77.5 ^{x}** *66.5; 93*	**73*^{x}** *70; 80*
			Heart rate (beat min^{-1})		
Sham-operated	**83.5** *71.1; 99.9*	**75.8** *66.3; 85*	**82.5** *67.8; 105.2*	**87.6** *75.6; 104.5*	**94.6** *76.1; 112*
Cardiac tamponade	**76.1** *64.5; 112*	**118.8*^{x}** *108.5; 144.1*	**110.9** *90.9; 120.5*	**115.8** *85.1; 128*	**125.1*** *102.1; 139.4*
Cardiac tamponade + methane	**80.3** *64; 105*	**114*^{x}** *108; 140.5*	**112.6*** *97; 134.5*	**112.6*** *98.5; 130*	**111** *88.5; 124*

Table 1. *Changes in haemodynamics. Cardiac index (L/min^{-1} m^{-2}), mean arterial pressure (mmHg) heart rate (beat min^{-1}). *P<0.05 within group vs. baseline values (Friedman test followed by Dunn's post-hoc test) and ^{x}P<0.05 vs. sham-operated group (Kruskal–Wallis test followed by Dunn's post-hoc test).*

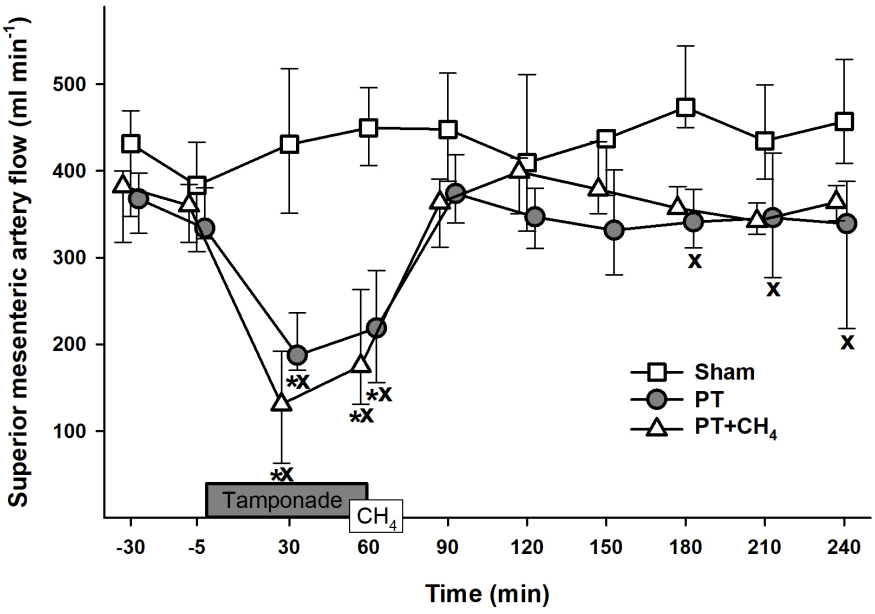

Figure 6. *Changes in superior mesenteric artery flow in the sham (n=6; white square-solid line), PT (n=6; grey circle-solid line) and PT+CH₄ (n=6; white triangle-solid line) groups.*

4.1.2. Changes in microcirculation

The RBCV did not change in the sham group, while a significant decrease from the baseline was detected in the PT and PT + CH₄-treated groups. At the end of the observation period, the CH₄-treated group showed a significant increase in RBCV compared to the non-treated PT group (Figure 7).

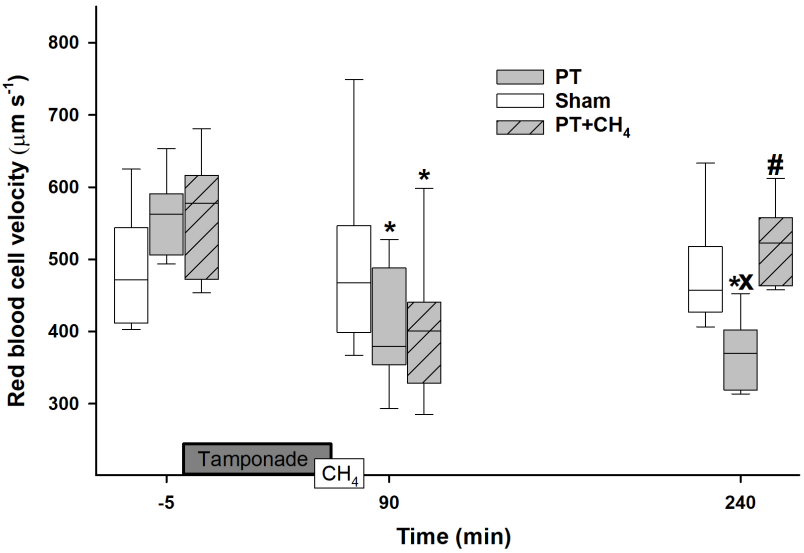

Figure 7. *Changes in red blood cell velocity in the sham (n=6; white box), PT (n=6; grey box) and PT+CH₄ (n=6; diagonal line in grey box) groups.*

4.1.3. Intestinal leukocyte accumulation

The leukocyte accumulation in the ileal tissue samples increased in the PT group compared to the sham group. The CH_4-treated group showed a significant decrease in the leukocyte accumulation compared to the non-treated PT group (Figure 8).

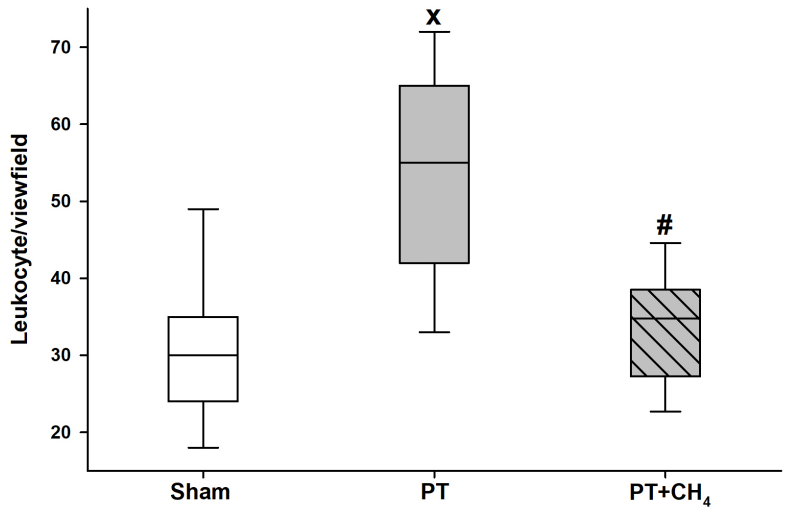

Figure 8. *Leukocyte content of the ileal biopsy in the sham (n=6; white box), PT (n=6; grey box) and PT+CH_4 (n=6; diagonal line in grey box) groups.*

4.1.4. Mucosal mast cell degranulation

The mast cell degranulation of the ileal tissue samples significantly increased after 90 minutes in the PT group and remained significantly high at the end of the observation period. This increase of degranulation was not observed in the CH_4-treated PT group at 90 minutes or at 240 minutes of the protocol (Figure 9).

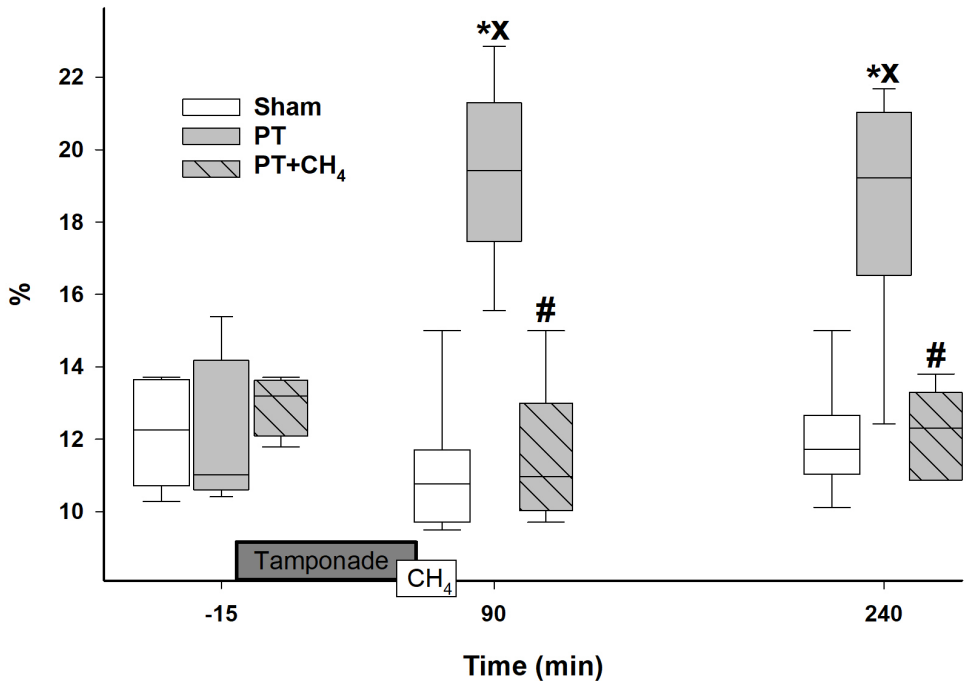

Figure 9. *Percentage of mast cell degranulation in the ileal biopsy in the sham (n=6; white box), PT (n=6; grey box) and PT+CH_4 (n=6; diagonal line in grey box) groups.*

4.1.5. *In vivo* histology

The mucosal morphology was examined with the intravital CLSEM technique in real time. The epithelial morphology of the small intestinal mucosa presented normal morphological patterns in the sham animals and in the baseline samples of the PT group and CH_4-treated group, while 30 min after PT induction longitudinal fissures appeared and partial epithelium defects were detected in the non-treated PT group. The lack of epithelium was extended in the end of observation. This extent of damage was not observed in the CH_4-treated PT group at 90 minutes or at 240 minutes (Figures 10AB). The scores of the mucosal damage were significantly higher in both non-treated and CH_4-treated groups at 90 min and 240 min of the experiment. However, CH_4 treatment significantly decreased the score of mucosal damage compared to the non-treated PT group (Figures 10AB).

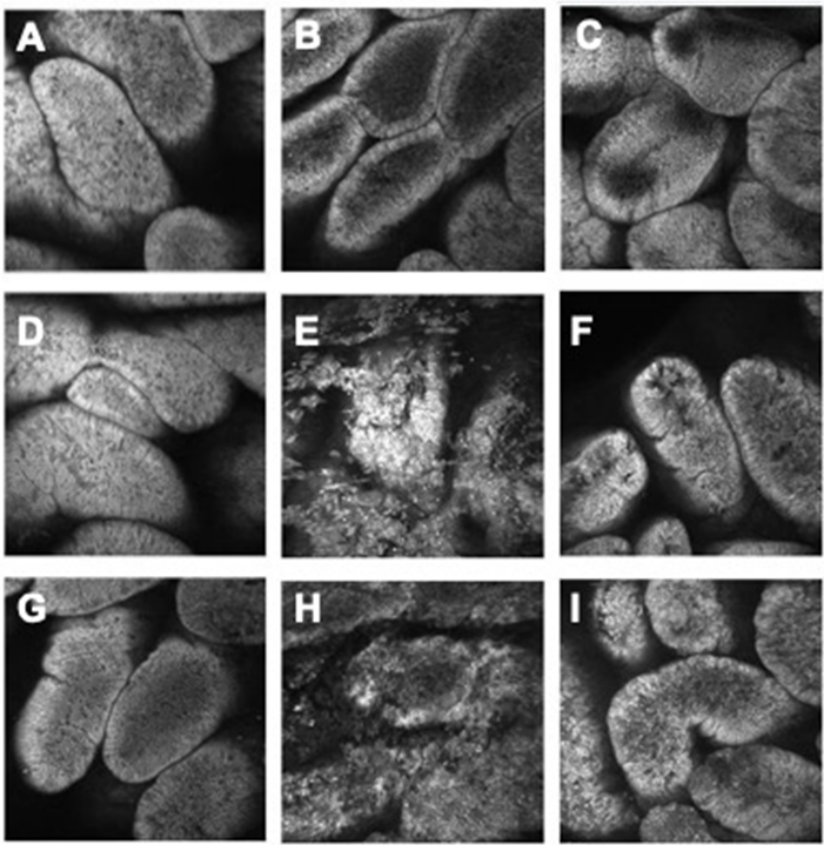

Figure 10A. In vivo *histology (CLSEM technique) showing the changes of the epithelial surface of the terminal ileum after acriflavine staining. The mucosal surface of the sham group (A, D, G), the structure of the mucosal surface in the PT group (B, E, H) and the structure of the mucosal surface in the PT+CH_4 group (C, F, I) are shown.*

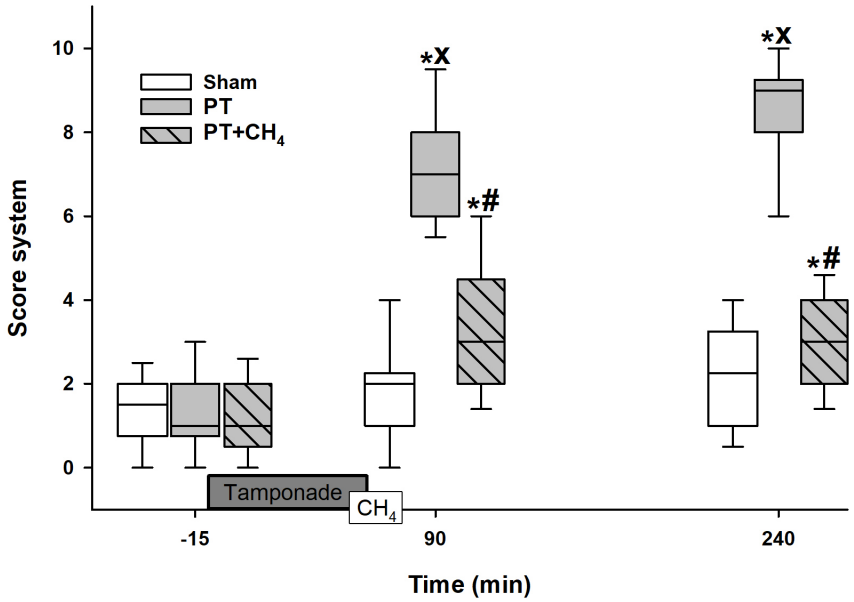

Figure 10B. *Changes in the values of scores of the* in vivo *histology in the sham (n=6; white box), PT (n=6; grey box) and PT+CH_4 (n=6; diagonal line in grey box) groups.*

4.1.6. Whole blood superoxide content

The superoxide content of the blood showed no difference in the baseline values for the three groups. After 30 min of the release of PT, the amount of superoxide significantly increased in the non-treated group compared to the sham group. In the CH_4-treated group, this increase was not observed. At 240 min significant differences in superoxide content could not be shown between the groups (Figure 11).

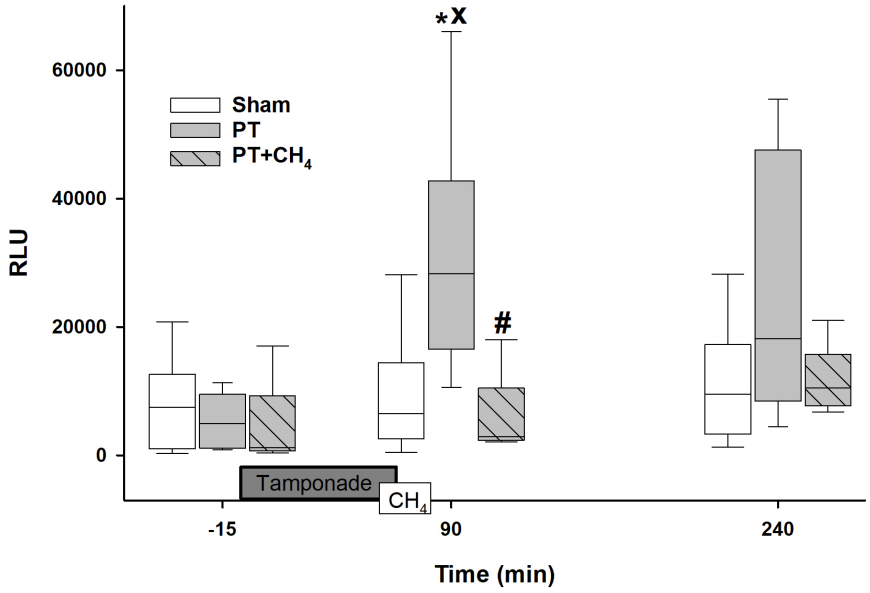

Figure 11. *Changes in whole blood superoxide production in the sham (n=6; white box), PT (n=6; grey box) and PT+CH_4 (n=6; diagonal line in grey box) groups.*

4.2. Results of Study II

4.2.1. Changes in renal arterial blood flow and hourly diuresis

A significantly decreased RA flow was detected during the CPB and post-CPB periods. CH_4 addition through the oxygenator resulted in significantly higher renal blood flow during the CPB period in contrast to the non-treated group (Figure 12A). The hourly diuresis during the observation period was significantly higher in the CH_4-treated group than in the animals without treatment (Figure 12B).

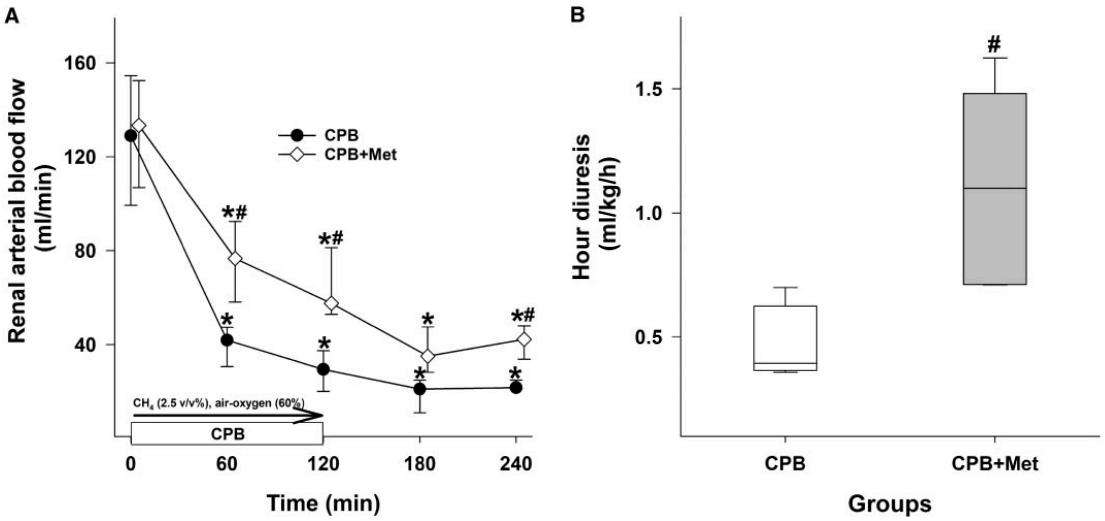

Figure 12. *Changes in renal artery blood flow **(A)** in the ECC (n=5; black circle with continuous line) and ECC+Met (n=5; empty diamond with solid line) groups. Hourly diuresis **(B)** in the ECC (empty box) and ECC+Met (grey box) groups. The plots demonstrate the median (horizontal line in the box) and the 25th and 75th percentiles. # $p < 0.05$ between the CH_4-treated and ECC groups (Mann–Whitney one-way analysis of variance on ranks).*

4.2.2. Changes in blood CH_4 level

The photoacoustic spectroscopy data showed a 1.4 ppm increase in CH_4 concentration in the aortic blood sample above the background CH_4 level. The CH_4 concentration, measured from the samples from the jugular vein, was significantly lower compared to the CH_4 levels in the aortic samples (Figure 13).

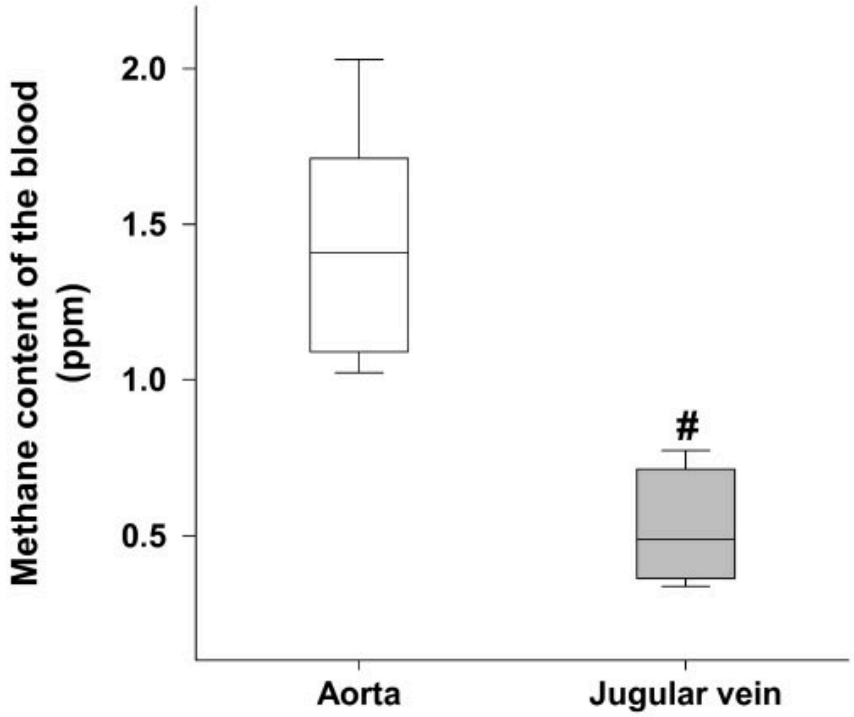

Figure 13. *CH_4 content of the blood in the aorta (empty box) and jugular vein (grey box).*

4.2.3. Changes in MPO activity

The rate of neutrophil accumulation in the intestinal, cardiac and renal tissue was determined by measurement of MPO activity. Intestinal MPO activity was significantly lower in the CPB–CH_4 group in contrast to the non-treated group (Figure 14A). The MPO level in the cardiac and renal tissue showed no differences between the two groups (Figures 14BC).

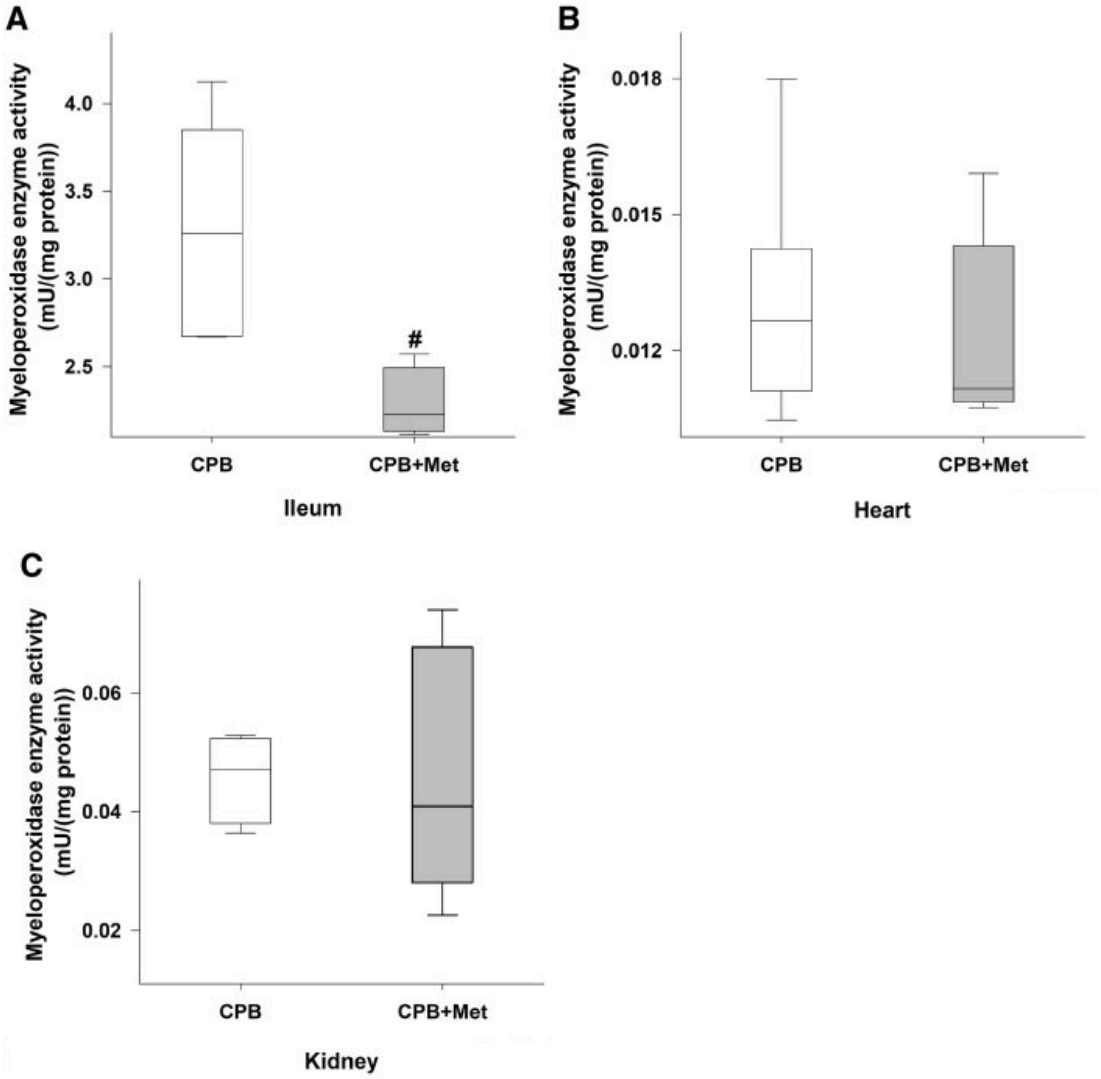

Figure 14. *Changes in small intestinal (A), cardiac (B) and renal (C) MPO activity in the ECC (n=5; empty box) and ECC+Met (n=5; grey box) groups.*

4.2.4. Changes in XOR activity

In the non-treated group, the XOR activity in all examined tissues was significantly higher 2 h after the CPB period compared to the values for the group with exogenous CH_4 administration (Figures 15ABC).

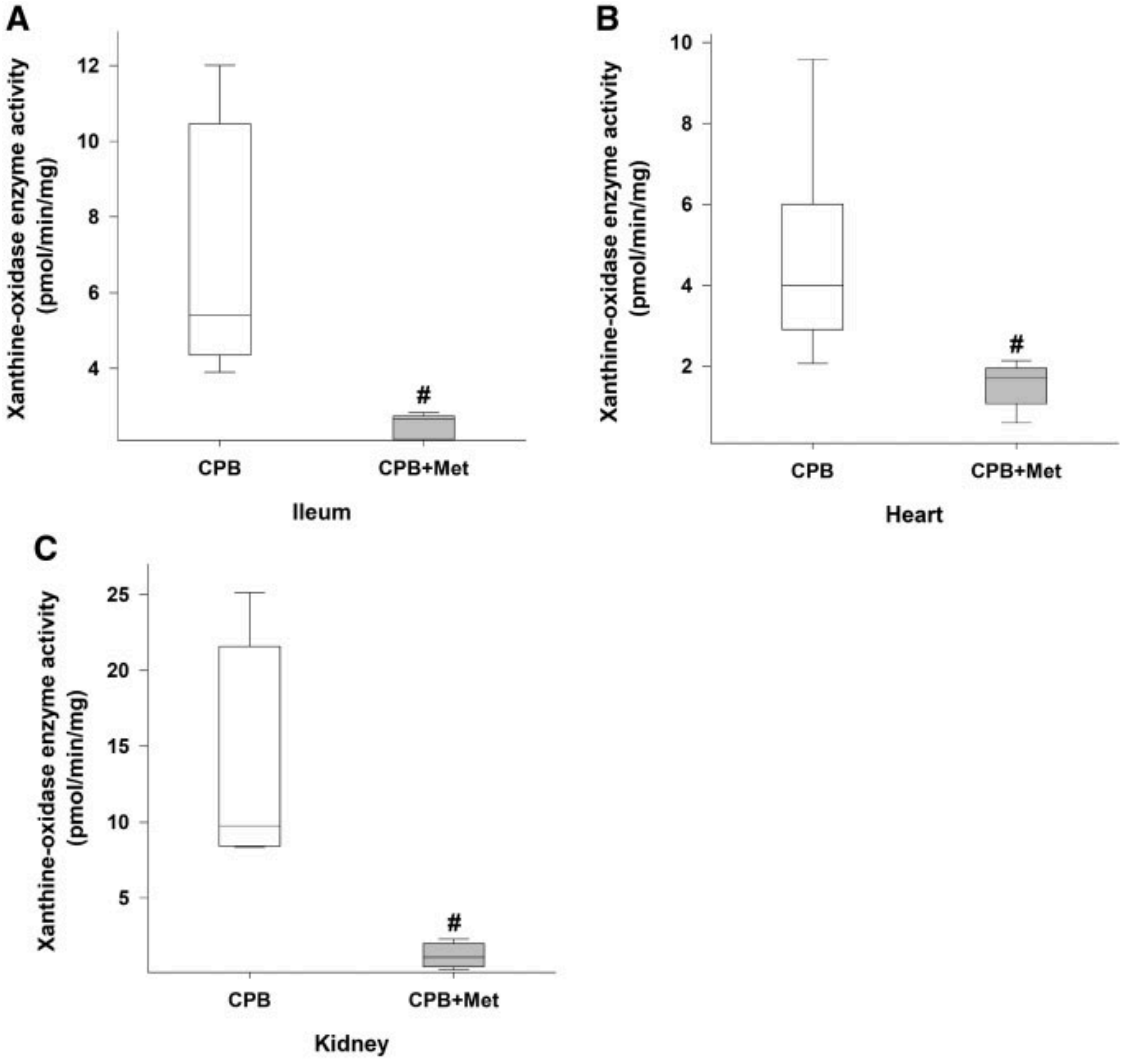

Figure 15. *Changes in small intestinal (A), cardiac (B) and renal (C) XOR activity in the ECC (n=5; empty box) and ECC+Met (n=5; grey box) groups.*

4.2.5. Changes in blood superoxide production

Whole blood superoxide production was reduced by CH_4 administration at the end of the experiment in contrast with the control CPB group (Figure 16).

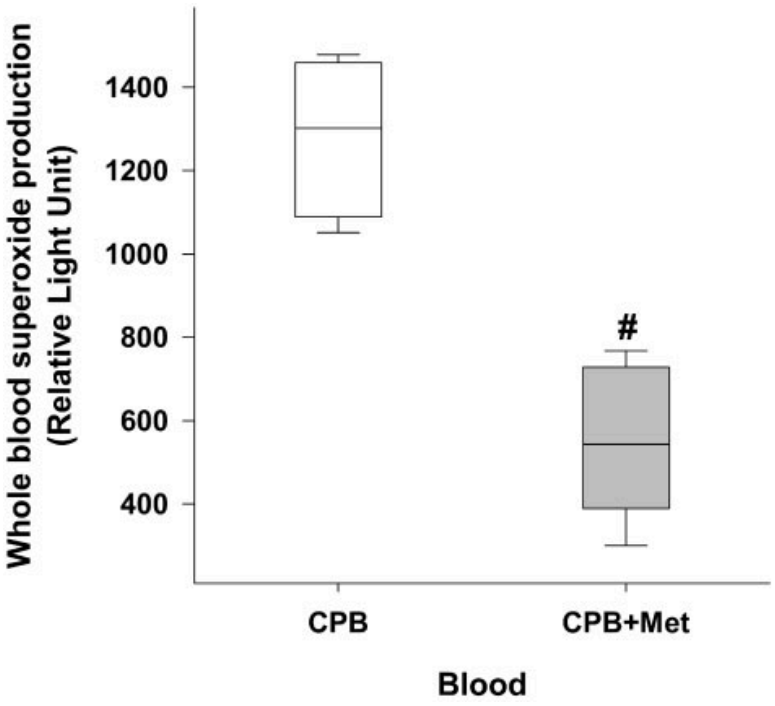

Figure 16. *Changes in whole blood superoxide production in the ECC (n=5; empty box) and ECC+Met (n=5; grey box) groups.*

4.2.6. Norepinephrine demand

During the post-CPB period, norepinephrine was administered to maintain a minimum of 60 mmHg MAP. We found significant differences between the inotropic demands of the 2 experimental groups. The CH_4-treated group required significantly less ($p = 0.006$) norepinephrine support compared to the non-treated group (Figure 17).

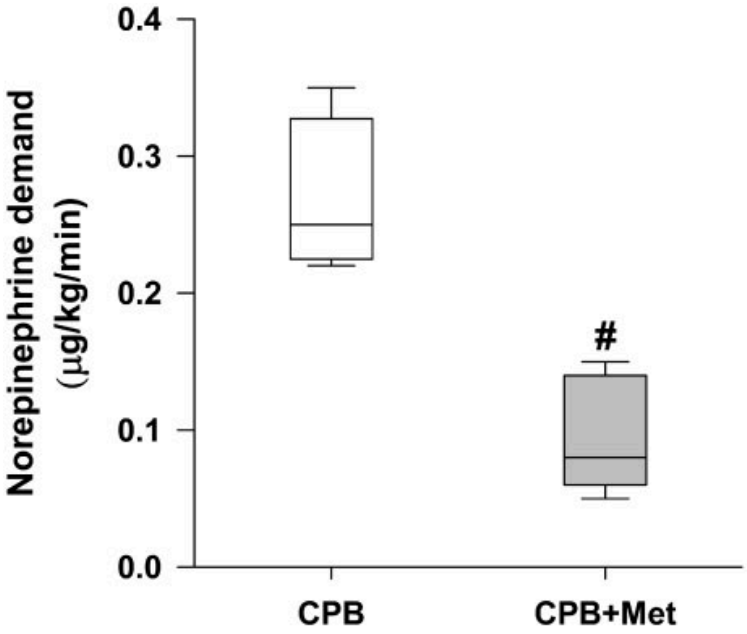

Figure 17. *Changes in norepinephrine demand in the ECC (n=5; empty box) and ECC+Met (n=5; grey box) groups.*

5. DISCUSSION

Cardiac surgery is a high-risk surgical category, where adverse circulatory events, including deterioration of intra-abdominal perfusion, can lead to excess morbidity and mortality. The main goal of this thesis was to model potentially harmful complications and consequences of clinical practice and to test possibilities of risk reduction with a novel, adjunctive treatment.

5.1. Study I

In the first protocol we investigated the overall characteristics and the mesenteric consequences of temporary mechanical compression of the heart leading to microcirculatory I-R of the splanchnic system. Experimental PT is a good model to study the pathomechanism of cardiogenic shock (32,56,65,66). but it has several limitations as well. The inherent disadvantage of the model is thoracotomy itself, the possibility of impaired lung function and the risk of bleeding. We attempted to improve the original model through several modifications. Most importantly, changing the species to swine (according to accepted ethical and legal requirements and standards) increased the translational power of the model. There are many anatomical similarities between the human and porcine heart (e.g. the structure of the coronary artery system and the lack of a collateral blood supply) and there are significant similarities, such as the NOS pathway, which is also almost identical in pigs and humans (67). A next, major forward step was the elimination of thoracotomy and the exclusive use of laparotomy for intestinal monitoring and pericardial cannula insertion (68)(69). In our new model, pledgets are placed in the pericardial purse-string suture line to seal the possible leaking points. This technique minimizes surgical trauma and may contribute to the stability of the experimental setting. Furthermore, we defined the importance of choosing the proper type of fluid to fill the pericardial sac. In the case of saline, the risk of fluid leakage and thus experimental instability is high; the technique was thus changed to the most relevant colloid, heparinized own blood drawn from the central venous line. The operative setup may not require special surgical skills, the tamponade can be easily induced, and the release of PT can be easily executed. It may therefore be a well-controllable model to investigate the inflammatory complications of central circulatory disturbances. The model is stable and repeatable, and these qualities may make it a good tool in the cardiovascular research arsenal.

The specific problem of low CO is often present in cardiac surgery, and there is a high demand for possible new therapeutic options with a solution for the

inflammatory consequences. Earlier studies have demonstrated the potential beneficial features of exogenous CH_4 in several I-R models, with the delivery of CH_4 by inhalation or *iv* administration of CH_4-enriched solutions (11)(12)(13)(17)(16). Therefore, we investigated the effects of a normoxic air-CH_4 mixture in a porcine model of PT-induced I-R damage with special emphasis on mucosal inflammatory reactions. To our knowledge, this translational approach has never been studied *in vivo* in the context of cardiac surgery.

The induction of PT significantly influenced the macrohaemodynamics. MAP and CO decreased, while CVP and HR rose. As a characteristic consequence of low CO, the mesenteric circulation deteriorated and the dramatic decrease of the SMA flow indicated the non-homogenous pattern of circulatory redistribution. The parallel *in viv*o detection of the microcirculation provided evidence for the decreased intestinal intramural perfusion. As expected, the haemodynamic disturbances were improved after the relief of the PT, but MAP and CO did not return to the normal baseline level. This circulatory state can be considered transitory, possibly returning to pre-PT values after longer observation times.

We detected no differences after CH_4 treatment in the macrohaemodynamics as compared to the non-treated control group. However, the RBCV in the mucosa significantly improved in the CH_4-treated group 180 min after the release of PT. These changes might be a consequence of the reduced pro-inflammatory activation, including the degranulation of MMCs, which might have an influence on peripheral vascular resistance.

Indeed, a higher proportion of activated mast cells were observed in the non-treated PT group 30 min after the relief of PT, and the same histological picture was seen after 240 min. In parallel, the accumulation of PMN leukocytes was also significant as a direct consequence of I-R. As discussed before, there is evidence that, in addition to IgE, non-immunologic G protein-coupled intracellular pathways play a vital role in I-R-derived MMC activation (46,47). Thus, the depletion of secretory granules and the release of various pro-inflammatory mediators could play a role in the recruitment of leukocytes. In line with the microcirculatory changes at 30 min after the release of PT, intravital CLSEM data also showed the first signs of structural damage of the mucosa. In line with the reduction of the presence and activation of pro-inflammatory cells, the extent of the structural damage to the mucosa was much lower and the content of superoxide in the blood was also reduced by CH_4 administration.

The available data on possible pathways of CH_4 effects (i.e. anti-inflammatory, antioxidant and anti-apoptotic) in various *in vitro* and *in vivo* experimental models were recently reviewed (9). It has been suggested that many effects can be explained with the physico-chemical properties of the non-polar gas. Until now no specific receptors or enzymes have been found mediating the CH_4 effects. However, there is evidence that CH_4 attenuates ROS production through the activation of antioxidant enzymes via the Nrf2-ARE pathway (70). As a result of Nrf2-ARE, the activation of downstream enzymes (i.e. haem oxygenase-1, catalase and superoxide dismutase) and lower production of ROS is expected, leading to anti-inflammatory effects. In addition to these intracellular signalling pathways, the mitochondrial electron transport system is believed to be a potential target of CH_4. Strifler et al. reported that leak mitochondrial respiration improved in a medium containing 2.2% CH_4–air mixture (71). These potential effects of CH_4 can be explained if CH_4 dissolves in mitochondrial membranes. It may thus influence membrane rigidity or change the conformity of trans-membrane proteins in the respiratory chain, leading to alterations in ROS production. Therefore, the reduction of the source of ROS, including a decreased level of leucocyte and mast cell activation, may be associated with improved microcirculation and the overall better structural status of the mucosal surface.

5.2. Study II

To date, many refinements have been made to improve the use of CPB in cardiac surgery. Biocompatible circuits, the advanced oxygenator and pump design (72) with shorter perfusion times have made postoperative patient recovery more successful than ever before. Nevertheless, some degree of systemic inflammation with an altered organ redox state still develops, and it is still not possible to overcome severe inflammatory responses completely. Complications more often arise after longer perfusion times or longer extracorporeal membrane oxygenation treatments. Blood contact with foreign surfaces immediately triggers the intrinsic activation of the coagulation cascade, leading to the broad activation of different pro-inflammatory cascades and the PMNs, and the resultant oxidative stress limits postoperative recovery (73)(74). The systemic inflammatory response syndrome was targeted by corticosteroids, but a large-scale study showed no significant consequence in terms of mortality and morbidity (75). Promising results have been achieved with cytokine adsorption techniques in intraoperative cardiac surgery, but other data have shown no reduction in the pro-inflammatory effect (76).

In our model, we present a novel method of delivering an effective anti-inflammatory gas to improve the consequences of SIRS after CBP. The aim was to simulate a centrally-cannulated extracorporeal bypass circuit for a relatively short period of time. The cannulation of CPB and that of central VA-ECMO are in this case nearly identical, but the air–blood interface in the venous reservoir, the use of an occlusive roller pump, the duration of the extracorporeal circulation, the degree of haemodilution and the lack of heparin-coated circuits rather resemble CPB. However, based on the practical experience that can be derived from the model, we can say that the induction of the inflammatory reaction due to extracorporeal circulation takes less time and the reaction is more pronounced as compared to the use of a less damaging ECMO circuit. We have shown that this technique is stable and repeatable and provides a clinically relevant animal model to study the consequences of CPB-induced inflammatory reactions. Renal function is frequently affected by CPB and there is therefore a constant search for renal protection methods. In the present study, we observed a significant decrease in renal arterial flow during and after CPB, and, despite a decrease, the flow was significantly higher in the CH_4-treated group than without the addition of CH_4. The increase also had a functional effect, as the hourly diuresis remained in the low normal range in the CH_4-treated group as compared to the oliguria in the animals which had not received CH_4 treatment.

According to findings reported by Vogel et al. (77), superoxide is capable of directly increasing Ca^{2+} influx in the smooth muscle cells of renal afferent arterioles, resulting in vasoconstriction, which may cause decreased renal blood flow. The establishment of CPB inevitably leads to a certain degree of hypoperfusion and activation of superoxide-producing enzymes such as NADPH-oxidase and XOR (73). The significance of the effect of CH_4 on oxidative stress enzymes is emphasized by the lower superoxide level in the blood samples in the CH_4-treated group. Another important finding of our study is the decreased XOR activity in the cardiac tissue after the addition of CH_4. During tissue ischaemia and reperfusion, XOR is a significant source of superoxide and a known contributor to oxidative stress. Allopurinol, a XOR inhibitor, has a protective effect against I-R injury in different organs. This effect was exploited in the case of the University of Wisconsin (UW) organ storage solution, the gold standard in kidney preservation (78). In the present study, CH_4 inhalation significantly decreased renal XOR activity, thus possibly exerting an effect on renal function similar to that of allopurinol. According to arterial and venous data, approximately 2/3 of the administered exogenous CH_4 was distributed across the body.

Since decreased XOR activity was detected in the cardiac and small intestinal samples as well, this points to a systemic, non-organ-specific effect of CH_4.

As discussed, the effects of CH_4 are possibly due to the physico-chemical properties of the gas (70)(71). Besides transport with the blood flow, the diffusion through cell membranes can provide biologically accessible CH_4 molecules, even in less perfused areas (dissolved in lipids, non-polar regions of proteins etc.). In addition, CH_4 treatment also reduced MPO activity in the small intestine, suggesting decreased leucocyte infiltration after CPB. Interestingly, this effect was absent in the heart and kidney, a finding which is consistent with the experimental findings reported by Murphy et al., who also noted the lack of PMN infiltration in the renal tissue 1.5 h after CPB in a similar, relatively short-term, non-recovery set-up (79). We suggest that the tissue-specific differences are due to the barrier nature and more pronounced immune function of the intestinal mucosa. Here, the baseline MPO values are approx. 2 magnitudes higher as compared to those of other tissues. On the other hand, as a shock organ, the GI tract is more exposed to the harmful effects of low flow and hypoxia caused by redistributed circulation during and after CPB; therefore, inflammatory activation may also be present on a much larger scale and in an earlier time frame. It should be noted that the inotropic demand was also significantly lower in CH_4-treated animals. Norepinephrine can influence renal perfusion; however, the doses that were administered in this study should not cause impairment of the renal circulation (80). Moreover, Schaer et al. (81) reported that norepinephrine treatment increased renal blood flow in dogs until the peak dose of 1.6 mg/kg/min, while the largest dose used in the present study was 0.35 mg/kg/min. Further, the effect of CH_4 treatment on renal flow was already observed 60 min after the start of CPB, thus ruling out the possible effect of inotropic treatment on this parameter.

5.3. Limitations

It is important to list the limitations of the studies. As pigs have immune responses and cardiac anatomical and functional similarities comparable to humans (82), in a study involving 4 species (i.e. rats, guinea pigs, swine and humans), the activity of XOR in the pig heart was in the same range as that in human cardiac tissue, and the response to allopurinol was also similar (83). Nonetheless, these animals were healthy, without any accompanying cardiovascular alterations, while humans undergoing cardiac surgical interventions and/or possible CPB use are usually in a severely impaired cardiovascular condition prior to surgery. As beneficial as it is to

have an experimental PT model similar to humans, the use of a swine PT model consists of numerous drawbacks due to the pathophysiologic characteristics of PT. PT is often a hyper-acute state and is developed due to an existing cardiac pathology (aortic dissection, cardiac surgery, intervention). It is therefore not possible to re-enact the influences of pre-existing cardiac pathology on animal models. Also, multiple-series, multiple-group experiments are difficult to carry out due to temporal and financial limitations. In addition, technical limitations were also present in the models. The CPB circuits used in cardiac operations have more complex tubing and use multiple roller pump modules for venting, cardiotomy suction and cardioplegia delivery. Moreover, cardiotomy suction aspirates blood from the surgical site, which has already been in contact with tissue factor; thus, significant cellular activation has already taken place. As the model lacked cardioplegia or any cardiac arrest, ischaemia of the cardiac tissue was not present, thus possibly influencing the effectiveness of the treatment. However, we provided evidence that CH_4 administration might improve the consequences of PT and CPB even under such circumstances.

6. SUMMARY OF NEW FINDINGS

1. We significantly refined a previous experimental technique and designed a new animal model, which resembles iatrogenic PT. For this purpose, the pericardium was accessed through the diaphragm via median laparotomy, and a cannula was fixed into the pericardial cavity with a pledgeted purse-string suture. Tamponade was induced and maintained by intrapericardial administration of heparinized own blood.
2. We designed a simplified, but clinically relevant large animal model of CPB-induced SIRS, where the haemodynamic and microcirculatory consequences of ECC can be studied in sufficient detail.
3. We confirmed the bioactivity of CH_4 in a large animal model of PT. The decreased ileal leukocyte infiltration and mast cell degranulation with the parallel reduction of blood superoxide concentrations demonstrate that exogenous CH_4 efficiently modulates the pathways of oxidative stress leading to reduced structural damage of the mucosa.
4. We demonstrated for the first time that CH_4 treatment is capable of increasing renal blood flow and hourly diuresis in the post-CBP period. We also provided evidence that the transmembrane diffusion of CH_4 using a commercially available hollow fibre membrane oxygenator is able to reduce the inflammatory activation (neutrophil accumulation and XOR activity) in peripheral tissues (i.e. heart, kidney and ileum) and the circulation as well (as evidenced by reduced blood superoxide content), which indicates that systemic CH_4 administration may be a feasible way to modulate ECC-induced ROS production.

7. REFERENCES

1. Wang R. Gasotransmitters: growing pains and joys. Trends Biochem Sci. 2014 May;39(5):227–32.

2. Crutzen PJ, Andreae MO. Biomass burning in the tropics: impact on atmospheric chemistry and biogeochemical cycles. Science. 1990 Dec 21;250(4988):1669–78.

3. Eckburg PB. Diversity of the Human Intestinal Microbial Flora. Science. 2005 Jun 10;308(5728):1635–8.

4. de Lacy Costello BPJ, Ledochowski M, Ratcliffe NM. The importance of methane breath testing: a review. J Breath Res. 2013 Mar 8;7(2):024001.

5. Keppler F, Schiller A, Ehehalt R, Greule M, Hartmann J, Polag D. Stable isotope and high precision concentration measurements confirm that all humans produce and exhale methane. J Breath Res. 2016 Jan 29;10(1):016003.

6. Keppler F, Hamilton JTG, McRoberts WC, Vigano I, Braß M, Röckmann T. Methoxyl groups of plant pectin as a precursor of atmospheric methane: evidence from deuterium labelling studies. New Phytol. 2008 Jun;178(4):808–14.

7. Lenhart K, Bunge M, Ratering S, Neu TR, Schüttmann I, Greule M, et al. Evidence for methane production by saprotrophic fungi. Nat Commun. 2012 Jan;3(1).

8. Althoff F, Jugold A, Keppler F. Methane formation by oxidation of ascorbic acid using iron minerals and hydrogen peroxide. Chemosphere. 2010 Jun;80(3):286–92.

9. Mészáros AT, Szilágyi ÁL, Juhász L, Tuboly E, Érces D, Varga G, et al. Mitochondria As Sources and Targets of Methane. Front Med. 2017 Nov 13;4.

10. Pimentel M, Lin HC, Enayati P, van den Burg B, Lee H-R, Chen JH, et al. Methane, a gas produced by enteric bacteria, slows intestinal transit and augments small intestinal contractile activity. Am J Physiol-Gastrointest Liver Physiol. 2006 Jun;290(6):G1089–95.

11. Boros M, Ghyczy M, Érces D, Varga G, Tőkés T, Kupai K, et al. The anti-inflammatory effects of methane*: Crit Care Med. 2012 Apr;40(4):1269–78.

12. Yao Y, Wang L, Jin P, Li N, Meng Y, Wang C, et al. Methane alleviates carbon tetrachloride induced liver injury in mice: anti-inflammatory action demonstrated by increased PI3K/Akt/GSK-3β-mediated IL-10 expression. J Mol Histol. 2017 Aug;48(4):301–10.

13. Ye Z, Chen O, Zhang R, Nakao A, Fan D, Zhang T, et al. Methane Attenuates Hepatic Ischemia/Reperfusion Injury in Rats Through Antiapoptotic, Anti-Inflammatory, and Antioxidative Actions: Shock. 2015 Aug;44(2):181–7.

14. Sun A, Wang W, Ye X, Wang Y, Yang X, Ye Z, et al. Protective Effects of Methane-Rich Saline on Rats with Lipopolysaccharide-Induced Acute Lung Injury. Oxid Med Cell Longev. 2017;2017:1–12.

15. Wang W, Huang X, Li J, Sun A, Yu J, Xie N, et al. Methane Suppresses Microglial Activation Related to Oxidative, Inflammatory, and Apoptotic Injury during Spinal Cord Injury in Rats. Oxid Med Cell Longev. 2017;2017:1–11.

16. Liu L, Sun Q, Wang R, Chen Z, Wu J, Xia F, et al. Methane attenuates retinal ischemia/reperfusion injury via anti-oxidative and anti-apoptotic pathways. Brain Res. 2016 Sep;1646:327–33.

17. Chen O, Ye Z, Cao Z, Manaenko A, Ning K, Zhai X, et al. Methane attenuates myocardial ischemia injury in rats through anti-oxidative, anti-apoptotic and anti-inflammatory actions. Free Radic Biol Med. 2016 Jan;90:1–11.

18. Song K, Zhang M, Hu J, Liu Y, Liu Y, Wang Y, et al. Methane-rich saline attenuates ischemia/reperfusion injury of abdominal skin flaps in rats via regulating apoptosis level. BMC Surg. 2015 Dec;15(1).

19. Shen M, Fan D, Zang Y, Chen Y, Zhu K, Cai Z, et al. Neuroprotective effects of methane-rich saline on experimental acute carbon monoxide toxicity. J Neurol Sci. 2016 Oct;369:361–7.

20. Meng Y, Jiang Z, Li N, Zhao Z, Cheng T, Yao Y, et al. Protective Effects of Methane-Rich Saline on Renal Ischemic-Reperfusion Injury in a Mouse Model. Med Sci Monit. 2018 Oct 31;24:7794–801.

21. Li Z, Jia Y, Feng Y, Cui R, Miao R, Zhang X, et al. Methane alleviates sepsis‐induced injury by inhibiting pyroptosis and apoptosis in vivo and in vitro experiments. :14.

22. Poles MZ, Bodi N, Bagyanszki M, Fekete E, Meszaros AT, Varga G, et al. Reduction of nitrosative stress by methane: Neuroprotection through xanthine oxidoreductase inhibition in a rat model of mesenteric ischemia-reperfusion. Free Radic Biol Med. 2018 May 20;120:160–9.

23. He R, Wang L, Zhu J, Fei M, Bao S, Meng Y, et al. Methane-rich saline protects against concanavalin A-induced autoimmune hepatitis in mice through anti-inflammatory and anti-oxidative pathways. Biochem Biophys Res Commun. 2016 Jan;470(1):22–8.

24. Jia Y, Li Z, Liu C, Zhang J. Methane Medicine: A Rising Star Gas with Powerful Anti-Inflammation, Antioxidant, and Antiapoptosis Properties. Oxid Med Cell Longev. 2018;2018:1–10.

25. Hauffe T, Krüger B, Bettex D et al. Shock Management For Cardio-Surgical ICU Patients — The Golden Hours. Card Fail Rev. 2015;1(2):75.

26. Carden DL, Granger DN. Pathophysiology of ischaemia-reperfusion injury. J Pathol. 2000 Feb;190(3):255–66.

27. Floyd RA, Carney JM. Free radical damage to protein and DNA: Mechanisms involved and relevant observations on brain undergoing oxidative stress. Ann Neurol. 1992;32(S1):S22–7.

28. Bari G, Érces D, Varga G, Szűcs S, Bogáts G. A pericardialis tamponád kórélettana, klinikuma és állatkísérletes vizsgálati lehetőségei. Orv Hetil. 2018 Feb;159(5):163–7.

29. Seferović PM, Ristić AD, Imazio M, Maksimović R, Simeunović D, Trinchero R, et al. Management strategies in pericardial emergencies. Herz Kardiovaskuläre Erkrank. 2006;31(9):891–900.

30. Orbach A, Schliamser JE, Flugelman MY, Zafrir B. Contemporary evaluation of the causes of cardiac tamponade: Acute and long-term outcomes. Cardiol J. 2016 Feb 26;23(1):57–63.

31. Adler Y, Charron P, Imazio M, Badano L, Barón-Esquivias G, Bogaert J, et al. 2015 ESC Guidelines for the diagnosis and management of pericardial diseases: The Task Force for the Diagnosis and Management of Pericardial Diseases of the European Society of Cardiology (ESC)Endorsed by: The European Association for Cardio-Thoracic Surgery (EACTS). Eur Heart J. 2015 Nov 7;36(42):2921–64.

32. Kaszaki J, Nagy S, Tarnoky K, Laczi F, Vecsernyes M, Boros M. Humoral changes in shock induced by cardiac tamponade. Circ Shock. 1989 Oct;29(2):143–53.

33. Day JRS, Taylor KM. The systemic inflammatory response syndrome and cardiopulmonary bypass. Int J Surg. 2005;3(2):129–40.

34. Millar JE, Fanning JP, McDonald CI, McAuley DF, Fraser JF. The inflammatory response to extracorporeal membrane oxygenation (ECMO): a review of the pathophysiology. Crit Care. 2016 Dec;20(1).

35. Boros M, Szalay L, Kaszaki J. Endothelin-1 induces mucosal mast cell degranulation and tissue injury via ET $_{A}$ receptors. Clin Sci. 2002 Sep 1;103(s2002):31S-34S.

36. Szabo A, Boros M, Kaszaki J, Nagy S. The role of mast cells in mucosal permeability changes during ischemia-reperfusion injury of the small intestine. Shock Augusta Ga. 1997 Oct;8(4):284–91.

37. Boros M, Kaszaki J, Ördögh B, Nagy S. Mast cell degranulation prior to ischemia decreases ischemia-reperfusion injury in the canine small intestine. Inflamm Res. 1999 Apr;48(4):193–8.

38. Bischoff SC. Mast cells in gastrointestinal disorders. Eur J Pharmacol. 2016 May;778:139–45.

39. Krystel-Whittemore M, Dileepan KN, Wood JG. Mast Cell: A Multi-Functional Master Cell. Front Immunol. 2016 Jan 6;6.

40. González-de-Olano D, Álvarez-Twose I. Mast Cells as Key Players in Allergy and Inflammation. J Investig Allergol Clin Immunol. 2018 Dec 9;28(6):365–78.

41. Heib V, Becker M, Taube C, Stassen M. Advances in the understanding of mast cell function. Br J Haematol. 2008 Sep;142(5):683–94.

42. Sibilano R, Frossi B, Pucillo CE. Mast cell activation: A complex interplay of positive and negative signaling pathways. Eur J Immunol. 2014 Sep;44(9):2558–66.

43. Johnzon C-F, Rönnberg E, Pejler G. The role of mast cells in bacterial infection. Am J Pathol. 2016;186(1):4–14.

44. Rivera-Nieves J, Gorfu G, Ley K. Leukocyte adhesion molecules in animal models of inflammatory bowel disease: Inflamm Bowel Dis. 2008 Dec;14(12):1715–35.

45. Chelombitko MA, Fedorov AV, Ilyinskaya OP, Zinovkin RA, Chernyak BV. Role of reactive oxygen species in mast cell degranulation. Biochem Mosc. 2016 Dec;81(12):1564–77.

46. He Z, Ma C, Yu T, Song J, Leng J, Gu X, et al. Activation mechanisms and multifaceted effects of mast cells in ischemia reperfusion injury. Exp Cell Res. 2019 Mar;376(2):227–35.

47. Kuehn HS, Gilfillan AM. G Protein-coupled receptors and the modification of FcεRI- mediated mast cell activation. 2007;19.

48. Ito BR, Engler RL, del Balzo U. Role of cardiac mast cells in complement C5a-induced myocardial ischemia. Am J Physiol-Heart Circ Physiol. 1993 May;264(5):H1346–54.

49. Gazoni LM, Walters DM, Unger EB, Linden J, Kron IL, Laubach VE. Activation of A1, A2A, or A3 adenosine receptors attenuates lung ischemia-reperfusion injury. J Thorac Cardiovasc Surg. 2010 Aug;140(2):440–6.

50. Neurath MF. Cytokines in inflammatory bowel disease. Nat Rev Immunol. 2014 Apr 22;14(5):329–42.

51. Harrison R. Physiological Roles of Xanthine Oxidoreductase. Drug Metab Rev. 2004 Jan;36(2):363–75.

52. Xi H, Schneider BL, Reitzer L. Purine Catabolism in Escherichia coli and Function of Xanthine Dehydrogenase in Purine Salvage. J Bacteriol. 2000 Oct 1;182(19):5332–41.

53. Kostić DA, Dimitrijević DS, Stojanović GS, Palić IR, Đorđević AS, Ickovski JD. Xanthine Oxidase: Isolation, Assays of Activity, and Inhibition. J Chem. 2015;2015:1–8.

54. Patel NN, Toth T, Jones C, Lin H, Ray P, George SJ, et al. Prevention of post-cardiopulmonary bypass acute kidney injury by endothelin A receptor blockade*: Crit Care Med. 2011 Apr;39(4):793–802.

55. Lluch S, Moguilevsky HC, Pietra G, Shaffer AB, Hirsch LJ, Fishman AP. A reproducible model of cardiogenic shock in the dog. Circulation. 1969;39(2):205–218.

56. Starr FL 3rd, Samphilipo MAJ, White RIJ, Anderson JH. A reproducible canine model of nonocclusive mesenteric ischemia. Invest Radiol. 1982 Feb;17(1):34–6.

57. Jungwirth B, de Lange F. Animal Models of Cardiopulmonary Bypass: Development, Applications, and Impact. Semin Cardiothorac Vasc Anesth. 2010 Jun;14(2):136–40.

58. Fujii Y, Shirai M, Inamori S, Takewa Y, Tatsumi E. A novel small animal extracorporeal circulation model for studying pathophysiology of cardiopulmonary bypass. J Artif Organs. 2015 Mar;18(1):35–9.

59. Madrahimov N, Boyle EC, Gueler F, Goecke T, Knöfel A-K, Irkha V, et al. Novel mouse model of cardiopulmonary bypass. Eur J Cardiothorac Surg. 2018 Jan 1;53(1):186–93.

60. Tuboly E, Szabó A, Erős G, Mohácsi á, Szabó G, Tengölics R, et al. Determination of endogenous methane formation by photoacoustic spectroscopy. J Breath Res. 2013 Nov 1;7(4):046004.

61. Kuebler WM, Abels C, Schuerer L. Measurement of neutrophil content in brain and lung tissue by a modified myeloperoxidase assay. Nt J Microcirc Clin Exp. 1996;(16):89–97.

62. Beckman JS, Parks DA, Pearson JD, Marshall PA, Freeman BA. A sensitive fluorometric assay for measuring xanthine dehydrogenase and oxidase in tissues. Free Radic Biol Med. 1989 Jan;6(6):607–15.

63. Zimmermann T, Schuster R, Lauschke G, Trausch M, Albrecht S, Kopprasch S, et al. Chemiluminescence response of whole blood and separated blood cells in cases of experimentally induced pancreatitis and MDTQ-DA—Trasylol—ascorbic acid therapy. Anal Chim Acta. 1991 Dec;255(2):373–81.

64. Kovács T, Varga G, Érces D, Tőkés T, Tiszlavicz L, Ghyczy M, et al. Dietary Phosphatidylcholine Supplementation Attenuates Inflammatory Mucosal Damage in a Rat Model of Experimental Colitis: Shock. 2012 Aug;38(2):177–85.

65. Érces D, Nógrády M, Nagy E, Varga G, Vass A, Süveges G, et al. Complement C5A Antagonist Treatment Improves the Acute Circulatory and Inflammatory Consequences of Experimental Cardiac Tamponade: Crit Care Med. 2013 Nov;41(11):e344–51.

66. Vass A, Süveges G, Érces D, Nógrády M, Varga G, Földesi I, et al. Inflammatory Activation after Experimental Cardiac Tamponade. Eur Surg Res. 2013;51(1–2):1–13.

67. Iselin CE, Ny L, Mastrangelo D, Felley-Bosco E, Larsson B, Alm P, et al. The nitric oxide pathway in pig isolated calyceal smooth muscle. Neurourol Urodyn. 1999;18(6):673–85.

68. Bari G, Szűcs S, Érces D et al. Experimental pericardial tamponade–translation of a clinical problem to its large animal model. Turk J Surg. 2018 Sep 28;34(3):205–11.

69. Bari G, Szűcs S, Érces D, Ugocsai M, Bozsó N, Balog D, et al. A cardiogen sokk modellezése pericardialis tamponáddal. Magy Seb. 2017 Dec;70(4):297–302.

70. Wang L, Yao Y, He R, Meng Y, Li N, Zhang D, et al. Methane ameliorates spinal cord ischemia-reperfusion injury in rats: Antioxidant, anti-inflammatory and anti-apoptotic activity mediated by Nrf2 activation. Free Radic Biol Med. 2017 Feb;103:69–86.

71. Strifler G, Tuboly E, Szel E, Kaszonyi E, Cao C, Kaszaki J, et al. Inhaled Methane Limits the Mitochondrial Electron Transport Chain Dysfunction during Experimental Liver Ischemia-Reperfusion Injury. PloS One. 2016;11(1):e0146363.

72. Nguyen BAV, Fiorentino F, Reeves BC, Baig K, Athanasiou T, Anderson JR, et al. Mini Bypass and Proinflammatory Leukocyte Activation: A Randomized Controlled Trial. Ann Thorac Surg. 2016 Apr;101(4):1454–63.

73. McDonald CI, Fraser JF, Coombes JS, Fung YL. Oxidative stress during extracorporeal circulation. Eur J Cardiothorac Surg. 2014 Dec 1;46(6):937–43.

74. Zakkar M, Guida G, Suleiman M-S, Angelini GD. Cardiopulmonary Bypass and Oxidative Stress. Oxid Med Cell Longev. 2015;2015:1–8.

75. Whitlock RP, Devereaux PJ, Teoh KH, Lamy A, Vincent J, Pogue J, et al. Methylprednisolone in patients undergoing cardiopulmonary bypass (SIRS): a randomised, double-blind, placebo-controlled trial. The Lancet. 2015 Sep;386(10000):1243–53.

76. Bernardi MH, Rinoesl H, Dragosits K, Ristl R, Hoffelner F, Opfermann P, et al. Effect of hemoadsorption during cardiopulmonary bypass surgery – a blinded, randomized, controlled pilot study using a novel adsorbent. Crit Care. 2016 Dec;20(1).

77. Vogel PA, Yang X, Moss NG, Arendshorst WJ. Superoxide Enhances Ca $^{2+}$ Entry Through L-Type Channels in the Renal Afferent Arteriole. Hypertension. 2015 Aug;66(2):374–81.

78. Pacher P. Therapeutic Effects of Xanthine Oxidase Inhibitors: Renaissance Half a Century after the Discovery of Allopurinol. Pharmacol Rev. 2006 Mar 1;58(1):87–114.

79. Murphy GJ, Lin H, Coward RJ, Toth T, Holmes R, Hall D, et al. An initial evaluation of post-cardiopulmonary bypass acute kidney injury in swine☆. Eur J Cardiothorac Surg. 2009 Nov;36(5):849–55.

80. Bellomo R, Giantomasso DD. Noradrenaline and the kidney: friends or foes? Crit Care Med.2001;5(6):5.

81. Schaer GL, Fink MP, Parrillo JE. Norepinephrine alone versus norepinephrine plus low-dose dopamine: enhanced renal blood flow with combination pressor therapy. Crit Care Med. 1985 Jun;13(6):492–6.

82. Meurens F, Summerfield A, Nauwynck H, Saif L, Gerdts V. The pig: a model for human infectious diseases. Trends Microbiol. 2012 Jan;20(1):50–7.

83. Janssen M, van der Meer P, de Jong JW. Antioxidant defences in rat, pig, guinea pig, and human hearts: comparison with xanthine oxidoreductase activity. Cardiovasc Res. 1993 Nov;27(11):2052–7.

8. ACKNOWLEDGEMENTS

I would like to express my gratitude to Professor Mihály Boros, Head of the Institute of Surgical Research, for granting me the opportunity to work in his department and for his scientific guidance.

I am also grateful to Gábor Bogáts, the Head of the Department of Cardiac Surgery, for his support in my scientific work.

I am especially grateful to my two supervisors, Gabriella Varga and Dániel Érces, for their continuous support and for introducing me to the world of scientific problems. Without their continuous work and never-ending encouragement, this thesis would never have been written.

I wish to express my thanks for the excellent technical assistance at the Institute of Surgical Research and for assistance I received from Ágnes Fekete, Csilla Mester, Nikolett Beretka, Éva Nagyiván, Andrea Bús, Ágnes Lilla Kovács, Péter Szabó, Károly Tóth and Péter Sárkány.

I would like to thank my family and my parents for their love, patience and trust.

The PhD thesis was funded by Hungarian National Research, Development and Innovation Office NKFIH-K120232 and NKFIH-K116861, IKOM GINOP-2.3.2-15-2016-00015 and UNKP 20391-3/ 2018 /FEKUSTRAT grants.

9. ANNEX